NASA TECHNICAL NOTE

NASA TN D-3011

NASA TN D-3011

EFFECT OF REARWARD BODY STRAKES ON THE TRANSONIC AERODYNAMIC CHARACTERISTICS OF AN UNSWEPT-WING FIGHTER AIRCRAFT

by C. Robert Carter

Langley Research Center
Langley Station, Hampton, Va.

NATIONAL AERONAUTICS AND SPACE ADMINISTRATION • WASHINGTON, D. C. • SEPTEMBER 1965

NASA TN D-3011

EFFECT OF REARWARD BODY STRAKES ON THE TRANSONIC AERODYNAMIC CHARACTERISTICS OF AN UNSWEPT-WING FIGHTER AIRCRAFT

By C. Robert Carter

Langley Research Center
Langley Station, Hampton, Va.

NATIONAL AERONAUTICS AND SPACE ADMINISTRATION

For sale by the Clearinghouse for Federal Scientific and Technical Information
Springfield, Virginia 22151 – Price $2.00

EFFECT OF REARWARD BODY STRAKES ON THE TRANSONIC AERODYNAMIC CHARACTERISTICS OF AN UNSWEPT-WING FIGHTER AIRCRAFT

By C. Robert Carter
Langley Research Center

SUMMARY

An investigation has been conducted in the Langley 8-foot transonic pressure tunnel to determine the effects of two rearward body strakes on the aerodynamic characteristics of an unswept-wing fighter aircraft through high angles of attack. The tests were conducted at Mach numbers from 0.50 to 1.03 and angles of attack from approximately 2° to 26° at angles of sideslip of 0°, 3°, and 6°.

The results of this investigation indicate that the addition of the two rearward body strakes had little effect on the aerodynamic characteristics. Specifically, the "pitch-up" lift coefficient (lift coefficient at which longitudinal instability occurs) was increased only slightly by the addition of the strakes. Also, in the region of the pitch-up lift coefficient, only very small increases in the lateral stability parameters occurred.

INTRODUCTION

In an attempt to improve the maneuvering and handling characteristics of an unswept-wing fighter aircraft, two fin-like radial strakes were added rearward of and beneath the trailing edge of the wings. This modification was intended to alter the aerodynamic characteristics and thus make possible a considerable shortening of the turning radius of the aircraft at subsonic speeds. The results of test flights indicated that the addition of the two strakes would provide additional maneuvering capability. Also, the handling characteristics of the aircraft improved in all regions of test flight, and no performance degradation was observed.

In conjunction with these experimental flights, a wind-tunnel investigation was proposed. Since ventral fins had been shown to provide some increase in directional stability (refs. 1 and 2), the effects of the strakes on the lateral stability parameters in the vicinity of the "pitch-up" lift coefficient were of considerable interest. Therefore, an investigation was conducted in the Langley 8-foot transonic pressure tunnel to determine the effects of extending the flight test envelope. Special attention was directed to the effect of the strakes on the pitch-up lift coefficient, with and without the use of leading-edge and trailing-edge flap deflections.

The investigation was conducted at Mach numbers from 0.50 to 1.03 and angles of attack from approximately 2° to 26° at angles of sideslip of 0°, 3°, and 6°. The Reynolds number per foot varied from 2.79×10^{6} to 3.76×10^{6}.

SYMBOLS

Measurements for this investigation were taken in the U.S. Customary System of Units. Equivalent values are indicated herein parenthetically in the International System (SI) in the interest of promoting use of this system in future NASA reports. Details concerning the use of SI, together with physical constants and conversion factors, are given in reference 3.

The results are referred to the stability-axis system with the exception of the lateral-stability parameters which are referred to the body-axis system. The moment reference center is located on the fuselage reference line at a point $3.338\bar{c}$ rearward of the nose as shown in figure 1.

b — wing span, 1.882 ft (57.36 cm)

$\bar{c}$ — wing mean aerodynamic chord, 0.819 ft (24.96 cm)

C_D — drag coefficient, $\frac{\text{Drag}}{qS}$

C_L — lift coefficient, $\frac{\text{Lift}}{qS}$

$C_{L\left(C_{m_{C_L}} = 0\right)}$ — pitch-up lift coefficient

C_l — rolling-moment coefficient, $\frac{\text{Rolling moment}}{qSb}$

C_{l_β} — effective-dihedral parameter (measured at $\beta \approx 3^{\circ}$), $\frac{\Delta C_l}{\Delta\beta}$, per deg

C_m — pitching-moment coefficient, $\frac{\text{Pitching moment}}{qS\bar{c}}$

$C_{m_{C_L}}$ — longitudinal-stability parameter, $\frac{\partial C_m}{\partial C_L}$

C_n — yawing-moment coefficient, $\frac{\text{Yawing moment}}{qSb}$

C_{n_β} — directional-stability parameter (measured at $\beta \approx 3^{\circ}$), $\frac{\Delta C_n}{\Delta\beta}$, per deg

C_Y side-force coefficient, $\frac{\text{Side force}}{qS}$

C_{Y_β} side-force parameter (measured at $\beta \approx 3^\circ$), $\frac{\Delta C_Y}{\Delta\beta}$, per deg

M free-stream Mach number

p_t stagnation pressure, lb/sq ft (N/m^2)

q free-stream dynamic pressure, lb/sq ft (N/m^2)

R Reynolds number per foot (per 30.5 cm)

S wing area including projected area through fuselage, 1.444 sq ft $(0.1342\ m^2)$

α angle of attack, deg

β angle of sideslip (positive when nose is to left), deg

δ_{le} deflection of leading-edge flaps, deg

δ_{te} deflection of trailing-edge flaps, deg

APPARATUS AND TESTS

Tunnel

This investigation was conducted in the Langley 8-foot transonic pressure tunnel which is a single-return-type tunnel with a rectangular test section. The upper and lower walls are slotted longitudinally to allow continuous operation through the transonic speed range with negligible effects of choking and blockage. Stagnation pressures can be controlled from approximately 1/4 to 2 atmospheres (25 to 203 kN/m^2).

Model

Tests were performed with a 0.0858-scale model of an unswept-wing fighter aircraft. A dimensional sketch of the model is shown in figure 1, and the geometric dimensions of the model are summarized in table I. Photographs of the model are presented in figures 2 and 3, and a sketch of the model installation in the Langley 8-foot transonic pressure tunnel is shown in figure 4.

The model was equipped with a wing having 18.1° sweep of the quarter-chord line, an aspect ratio of 2.45, a taper ratio of 0.377, and a modified biconvex cross section. The wing was set at zero incidence to the fuselage reference line and had 10° negative geometric dihedral. The horizontal tail was fixed at zero incidence and the vertical tail had a 35° sweep of the quarter-chord line. The model was not equipped with internal ducting and the side inlets were faired into the contour of the body.

The wing was equipped with leading-edge and trailing-edge flaps which could be deflected from 0° to 15°. A drawing of the wing and the flaps is shown in figure 5. The rearward body strakes used in the investigation were fixed on the fuselage at 2° incidence. The strake details are shown in figure 6.

Test Conditions

Tests were conducted over a Mach number range from 0.50 to 1.03 and through angles of attack from approximately 2° to 26° at angles of sideslip of 0°, 3°, and 6°. Data over the Mach number range were obtained at a stagnation temperature of 120° F (322° K) and at a dewpoint such that the results were free of condensation effects. The variations of test dynamic pressure, stagnation pressure, and Reynolds number per foot (per 30.5 cm) with Mach number are shown in figure 7.

Corrections and Accuracy

Drag data presented herein are adjusted for the effects of model base and chamber pressure. The angles of attack and sideslip are corrected for model-sting and balance deflection due to aerodynamic forces and moments on the model. An additional correction for tunnel airflow angularity has been applied to the angle of attack. The effects of wind-tunnel boundary-reflected disturbances were negligible at all test Mach numbers except at a Mach number of 1.03, where a very weak reflected disturbance existed but had little effect on the data.

The estimated accuracies of the data (for low angles of attack) at a Mach number of 0.90 and a stagnation pressure of 1858 lb/sq ft (88.96 kN/m^2), based on instrument calibration and data repeatability, are within the following limits:

C_L	±0.013
C_D	±0.0007
C_m	±0.004
C_l	±0.003
C_n	±0.0009
C_Y	±0.003

The Mach number is estimated to be accurate within ±0.003; the angles of attack and angles of sideslip, within $\pm 0.1^{\circ}$.

PRESENTATION OF RESULTS

The results of this investigation are presented in the following figures:

DISCUSSION

The basic results of this investigation are presented in figures 8 to 12. The effects of the strakes on the "pitch-up" lift coefficient $C_{L\left(C_{m_{C_L}} = 0\right)}$ are summarized in figure 13. Addition of the strakes increased the pitch-up lift coefficient only very slightly. A summary of the effects of the wing flap deflections on the pitch-up lift coefficient is shown in figure 14. The configuration with $\delta_{le} = 5^{\circ}$ and $\delta_{te} = 10^{\circ}$ was the most effective in increasing the pitch-up lift coefficient over the test Mach number range, although the configuration with $\delta_{le} = 10^{\circ}$ and $\delta_{te} = 15^{\circ}$ was equally effective at the highest Mach number. In order to determine the effect of the strakes on the lateral characteristics in the region just before the pitch-up in the curve for C_m as a function of C_L, an angle of attack of 12° was chosen. The addition of the strakes resulted in only very slight increases in the lateral stability parameters, as summarized in figure 15.

CONCLUDING REMARKS

An investigation has been conducted in the Langley 8-foot transonic pressure tunnel to determine the effects of two rearward body strakes on the aerodynamic characteristics of an unswept-wing fighter aircraft through high angles of attack. The tests were conducted at Mach numbers from 0.50 to 1.03 and angles of attack from approximately 2° to 26° at angles of sideslip of 0°, 3°, and 6°.

The results of this investigation indicate that the addition of the two rearward body strakes had little effect on the aerodynamic characteristics. Specifically, the "pitch-up" lift coefficient (lift coefficient at which longitudinal instability occurs) was increased only slightly by the addition of the strakes. Also, in the region of the pitch-up lift coefficient, only very small increases in the lateral stability parameters occurred.

Langley Research Center,
National Aeronautics and Space Administration,
Langley Station, Hampton, Va., June 18, 1965.

REFERENCES

1. Holtzclaw, Ralph W.: Wind-Tunnel Investigation of Devices to Improve Static Directional Stability of an Unswept-Wing Airplane Model at Mach Numbers From 0.8 to 2.2. NASA MEMO 10-4-58A, 1958.

2. Spearman, M. Leroy; and Driver, Cornelius: Longitudinal and Lateral Stability Characteristics of a Low-Aspect-Ratio Unswept-Wing Airplane Model at Mach Numbers of 1.82 and 2.01. NACA RM L56H06, 1957.

3. Mechtly, E. A.: The International System of Units - Physical Constants and Conversion Factors. NASA SP-7012, 1964.

TABLE I.- GEOMETRIC CHARACTERISTICS OF MODEL

Wing:	
Area, sq ft (cm^2)	1.444 (1342)
Span, ft (cm)	1.882 (57.4)
Mean aerodynamic chord, ft (cm)	0.819 (24.9)
Aspect ratio	2.45
Taper ratio	0.377
Sweep of leading edge, deg	26.96
Sweep of quarter-chord line, deg	18.1
Incidence, deg	0
Dihedral, deg	-10
Airfoil section	Modified biconvex
Horizontal tail:	
Area, sq ft (cm^2)	0.355 (329.8)
Span, ft (cm)	1.022 (31.2)
Mean aerodynamic chord, ft (cm)	0.379 (11.6)
Aspect ratio	2.94
Taper ratio	0.311
Incidence, deg	0
Dihedral, deg	0
Sweep of quarter-chord line, deg	10.12
Airfoil section -	
Root	Modified 4.94-percent-thick biconvex
Tip	Modified 2.61-percent-thick biconvex
Vertical tail:	
Area, sq ft (cm^2)	0.258 (239.7)
Span, ft (cm)	0.475 (14.5)
Mean aerodynamic chord, ft (cm)	0.590 (17.9)
Sweep of quarter-chord line, deg	35
Airfoil section -	
Root	Modified biconvex
Tip	Flat sides $0.3\bar{c}$ to $0.7\bar{c}$
Ventral fin:	
Length, ft (cm)	0.668 (20.4)
Leading-edge sweep, deg	11.67
Area, sq ft (cm^2)	0.046 (42.7)
Fuselage:	
Length, ft (cm)	4.67 (142.3)
Maximum frontal area, sq ft (cm^2)	0.175 (162.6)
Rearward body strakes:	
Length, ft (cm)	0.406 (12.4)
Incidence, deg	2.0
Area -	
Planform, sq ft (cm^2)	0.025 (23.2)
Wetted, sq ft (cm^2)	0.0503 (46.7)
Leading-edge flaps:	
Area (each), sq ft (cm^2)	0.059 (54.8)
Length (chord), ft (cm)	0.606 (18.5)
Deflection angle, deg	0, 10, 15
Trailing-edge flaps:	
Area (each), sq ft (cm^2)	0.086 (79.9)
Length (chord), ft (cm)	0.393 (11.9)
Deflection angle, deg	0, 5, 10, 15

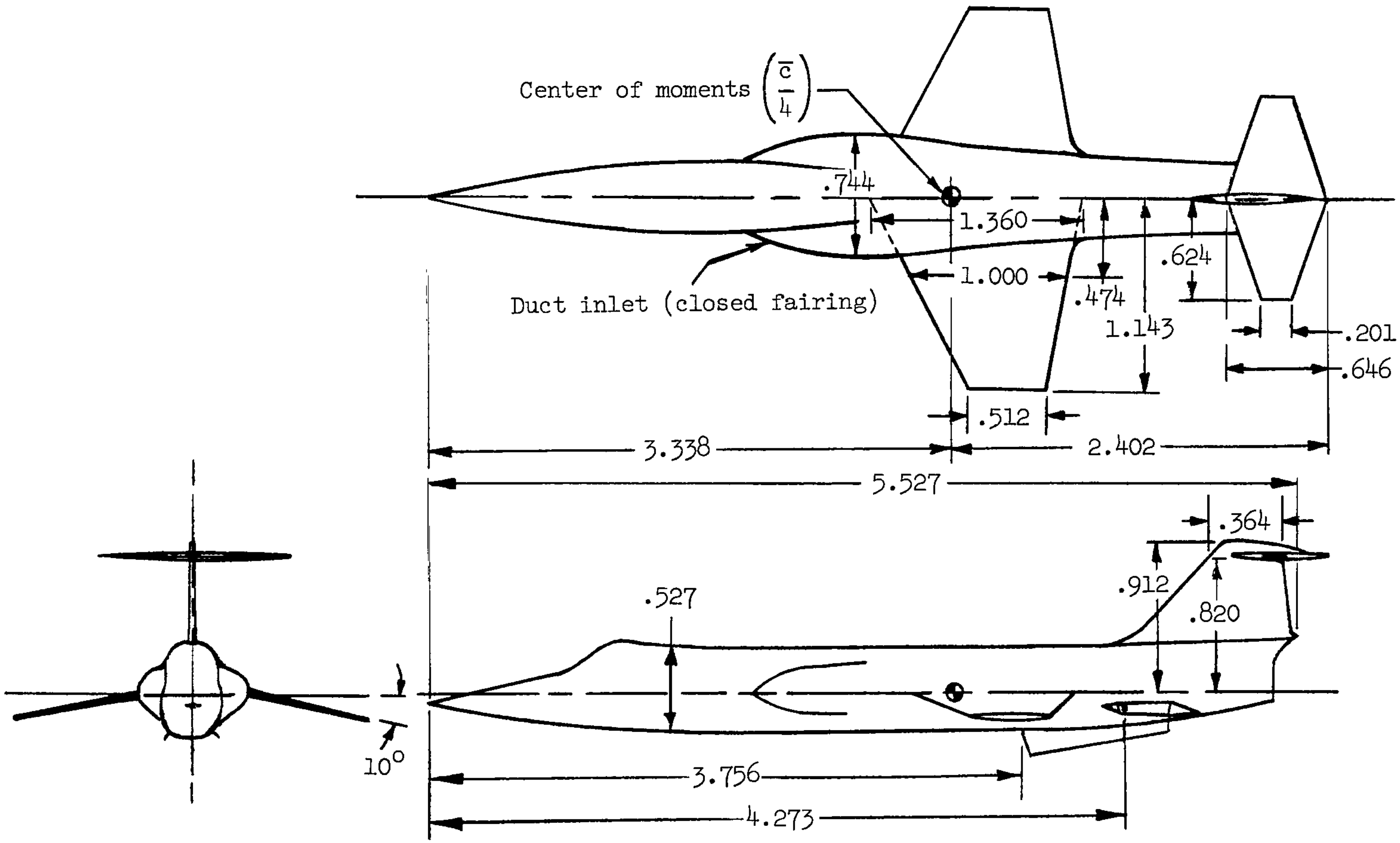

Figure 1.- Sketch of the model. Dimensions have been nondimensionalized with respect to the mean aerodynamic chord, $\bar{c}$ = 9.833 inches (24.976 cm).

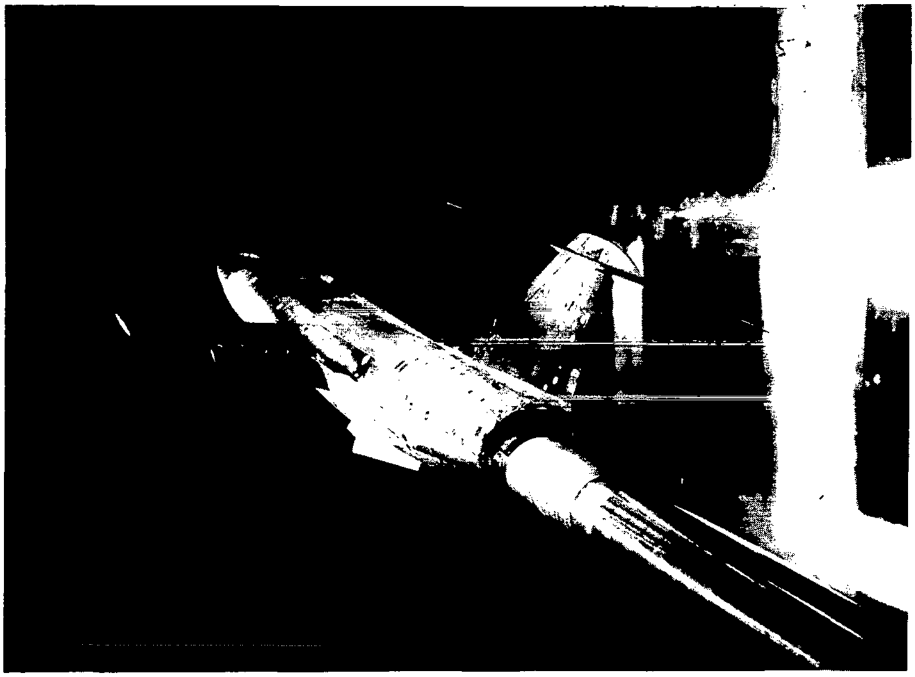

L-64-6005

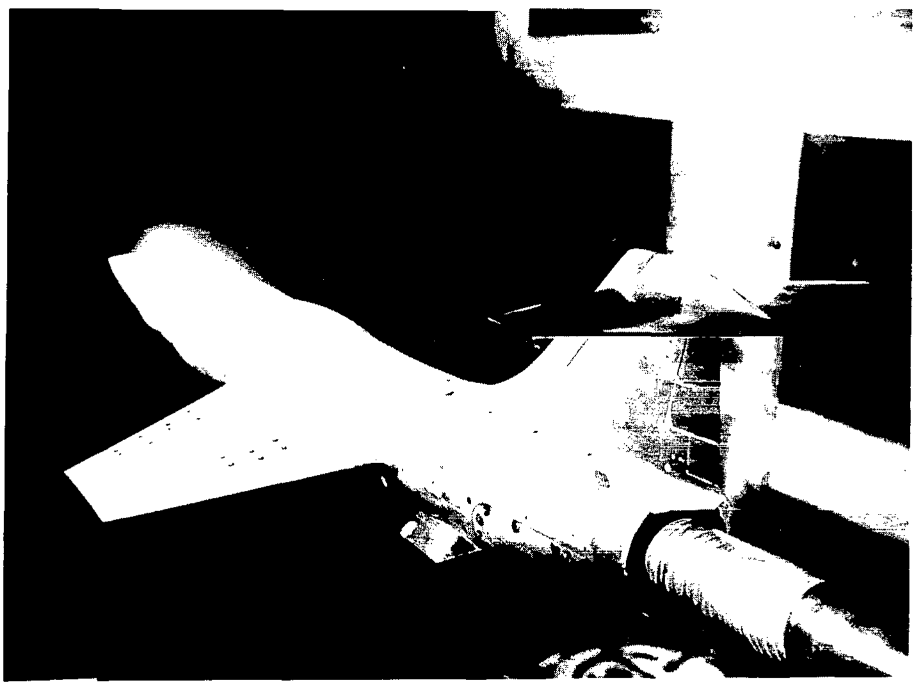

L-64-6009

Figure 2.- Photographs of the model installation in the Langley 8-foot transonic pressure tunnel.

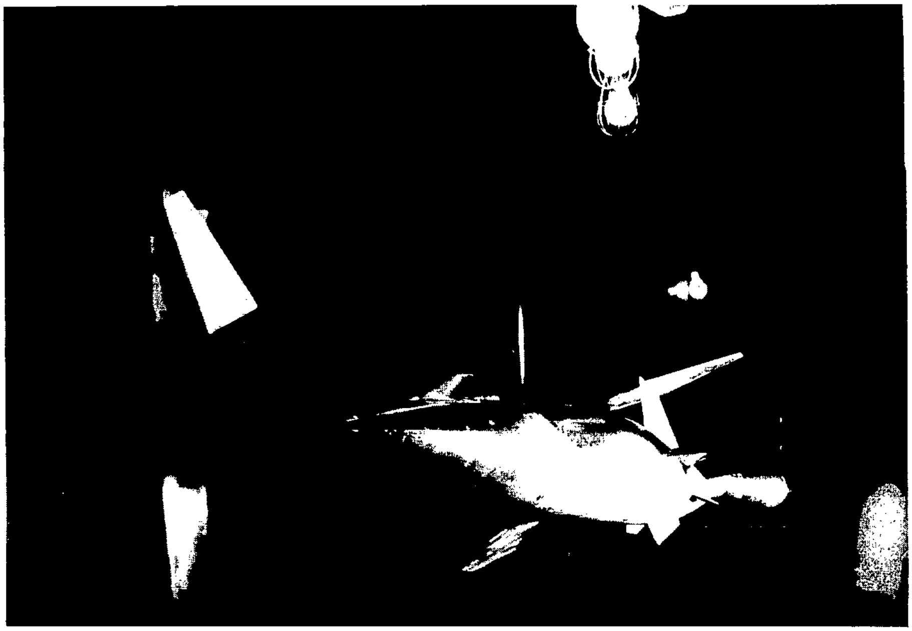

L-64-6007

Figure 3.- Photographs of the model showing strake details. L-64-6008

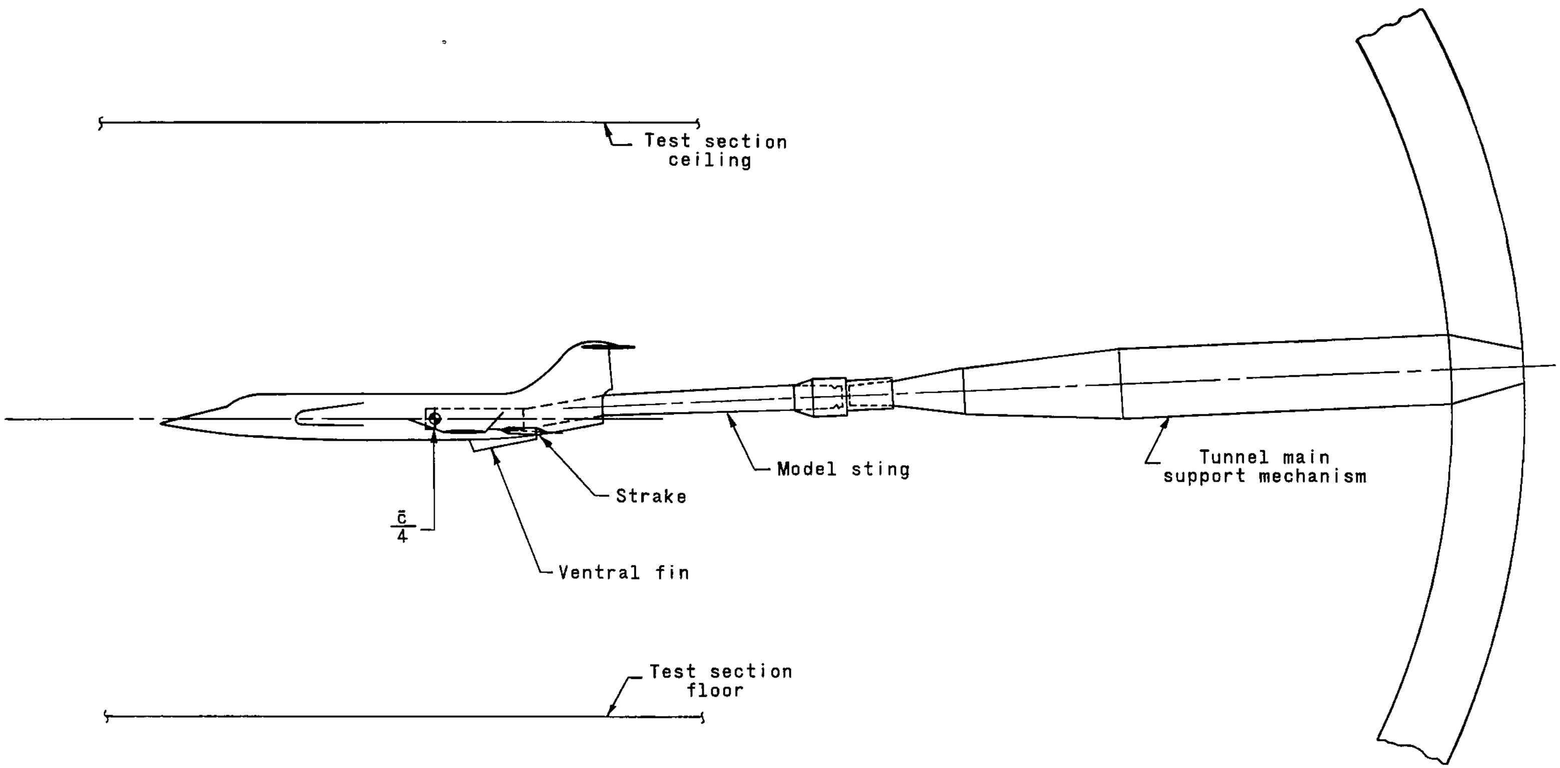

Figure 4.- Sketch of the model installation in the Langley 8-foot transonic pressure tunnel.

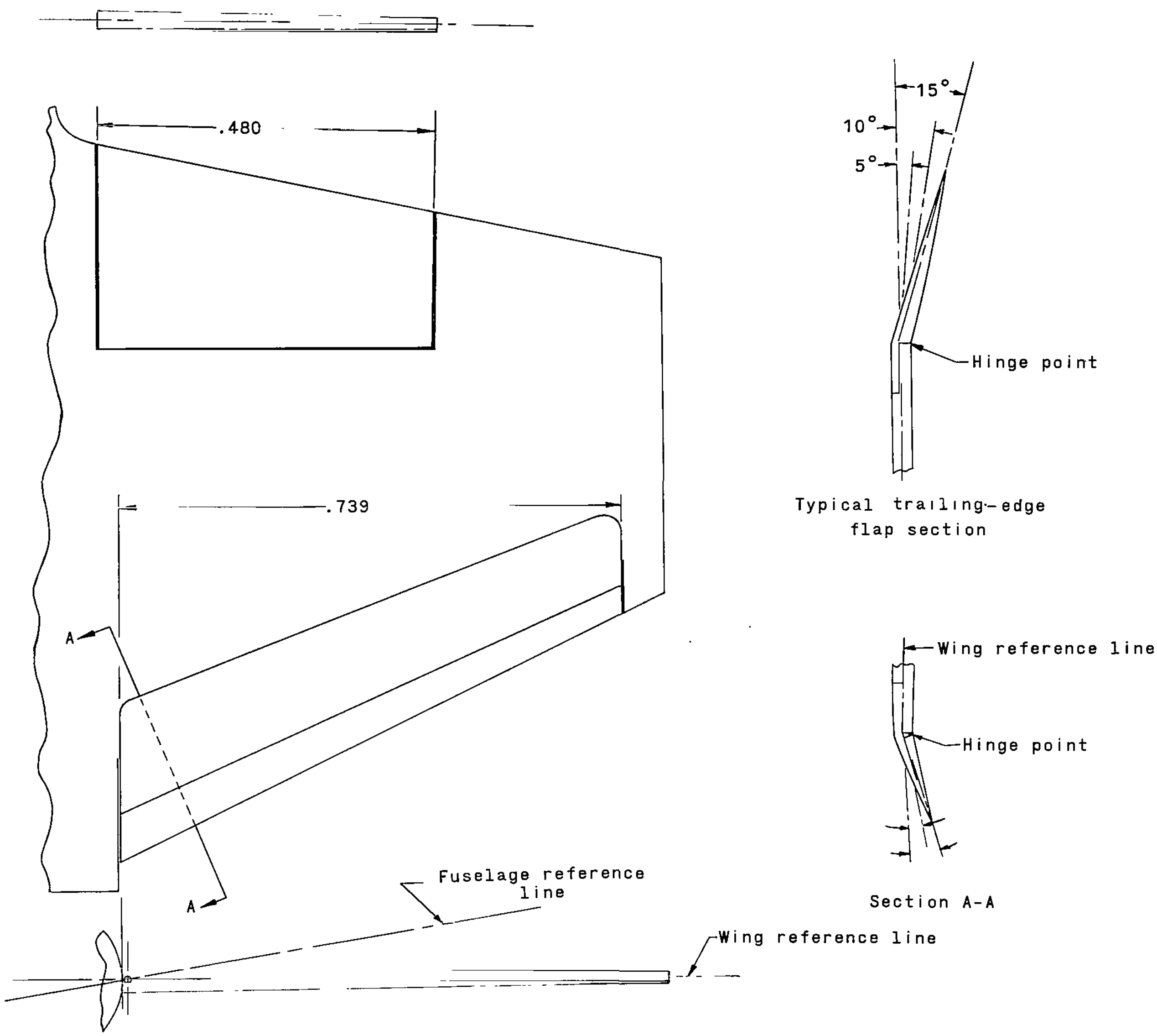

Figure 5.- Drawing of the wing showing leading-edge and trailing-edge flap details. Dimensions have been nondimensionalized with respect to the mean aerodynamic chord, $\bar{c}$ = 9.833 inches (24.976 cm).

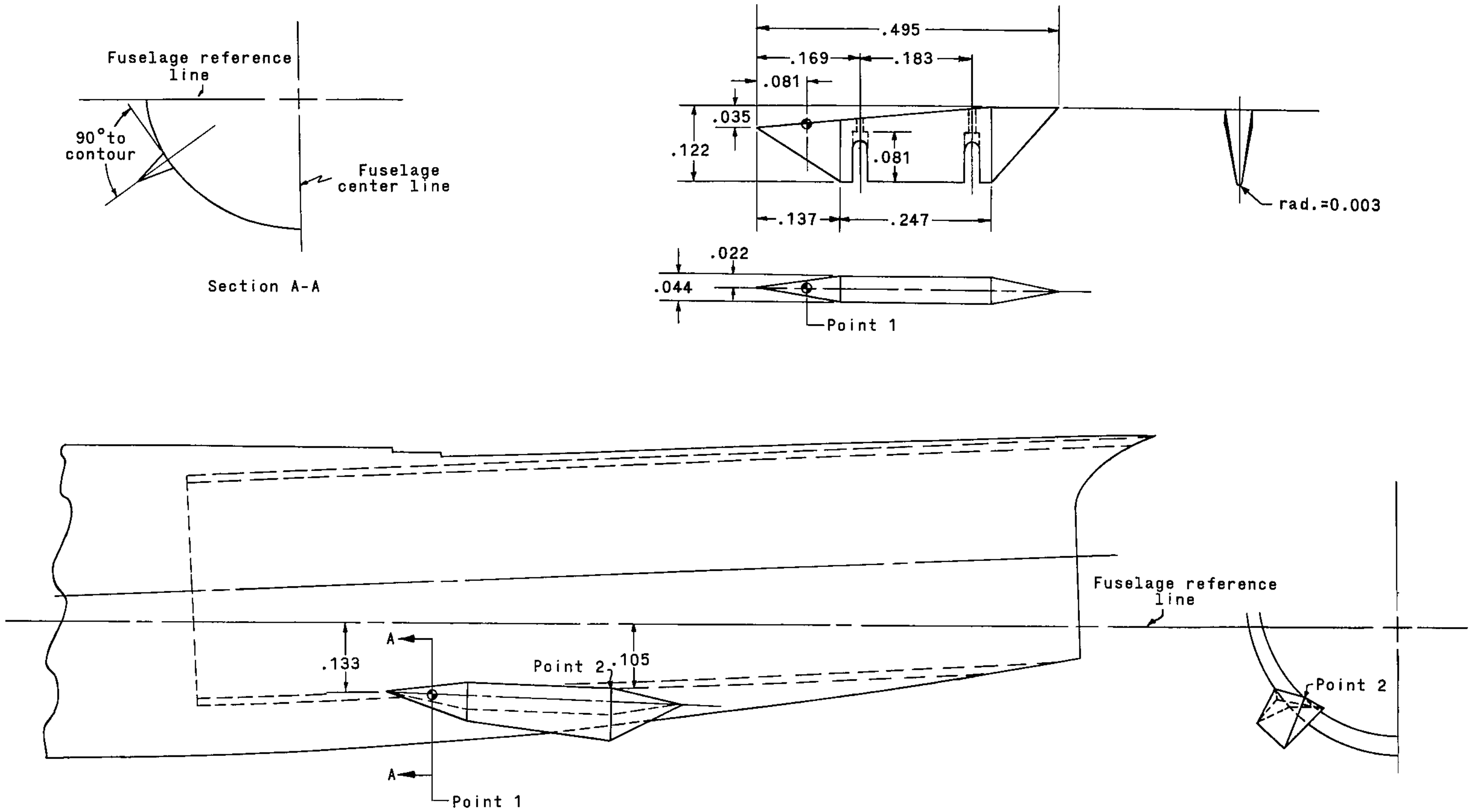

Figure 6.- Strake details. Dimensions have been nondimensionalized with respect to the mean aerodynamic chord, $\bar{c}$ = 9.833 inches (24.976 cm).

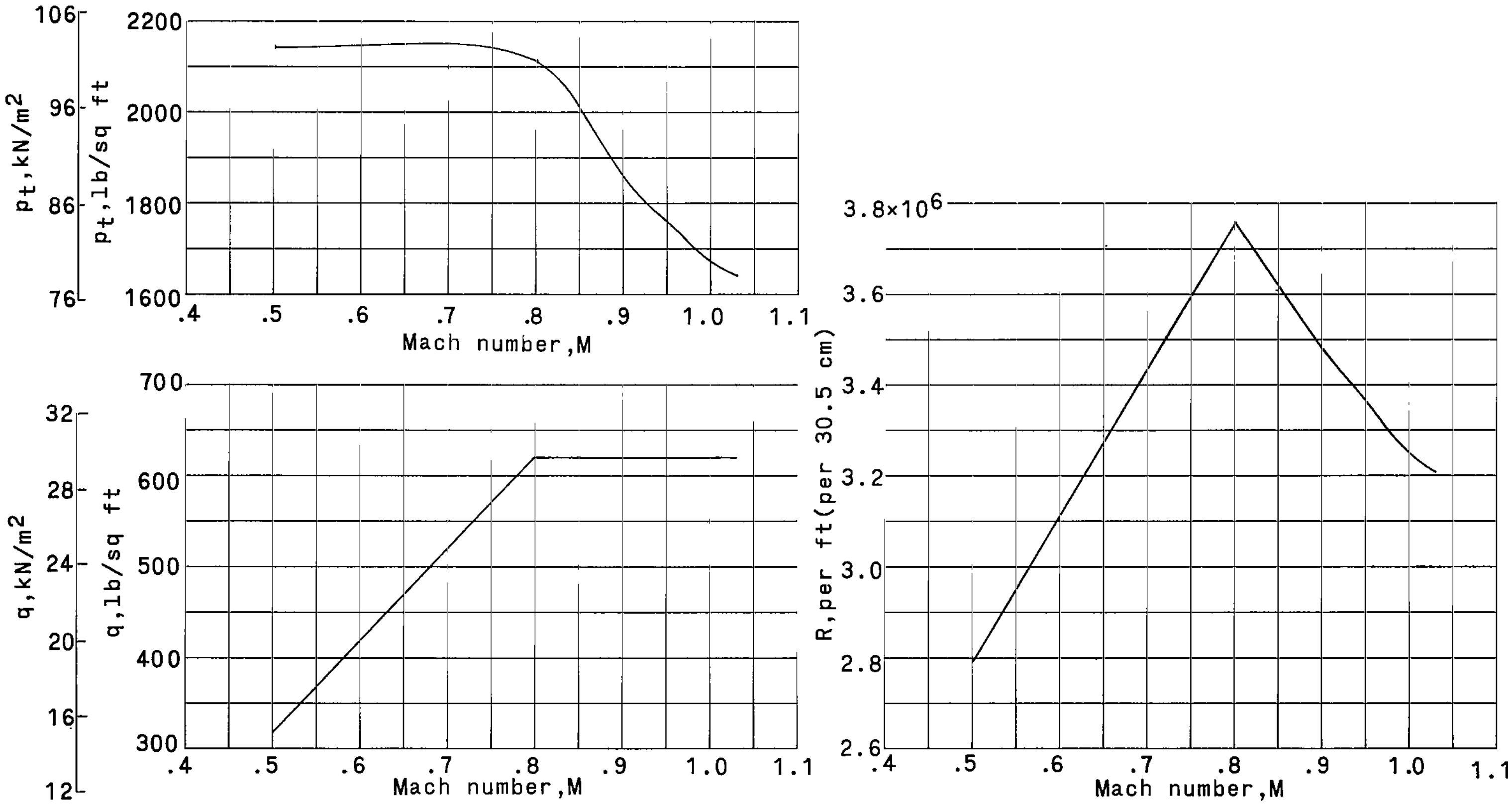

Figure 7.- Variation of stagnation pressure, dynamic pressure, and Reynolds number per foot (per 30.5 cm) with Mach number.

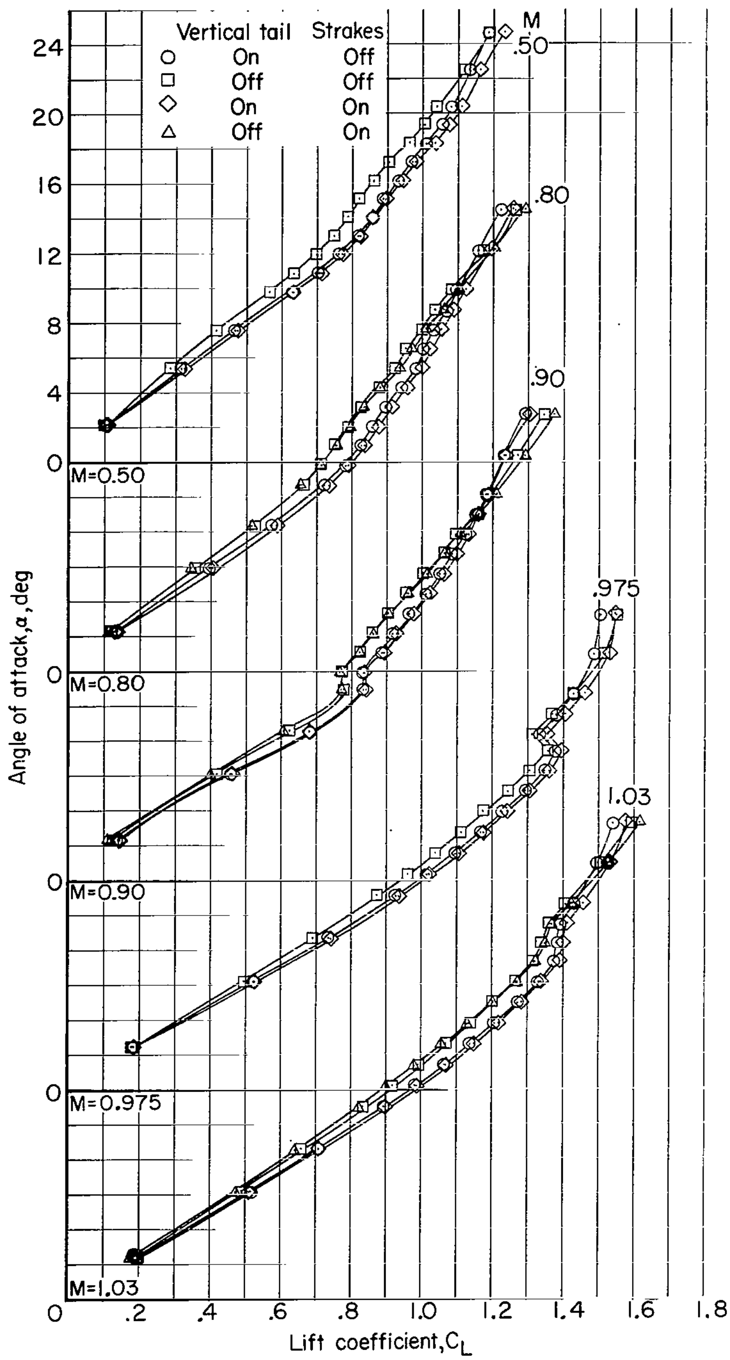

(a) Variation of α with C_L.

Figure 8.- Effects of the vertical tail and strakes on the aerodynamic characteristics of the configuration with leading-edge and trailing-edge flaps neutral. $\beta = 0^0$.

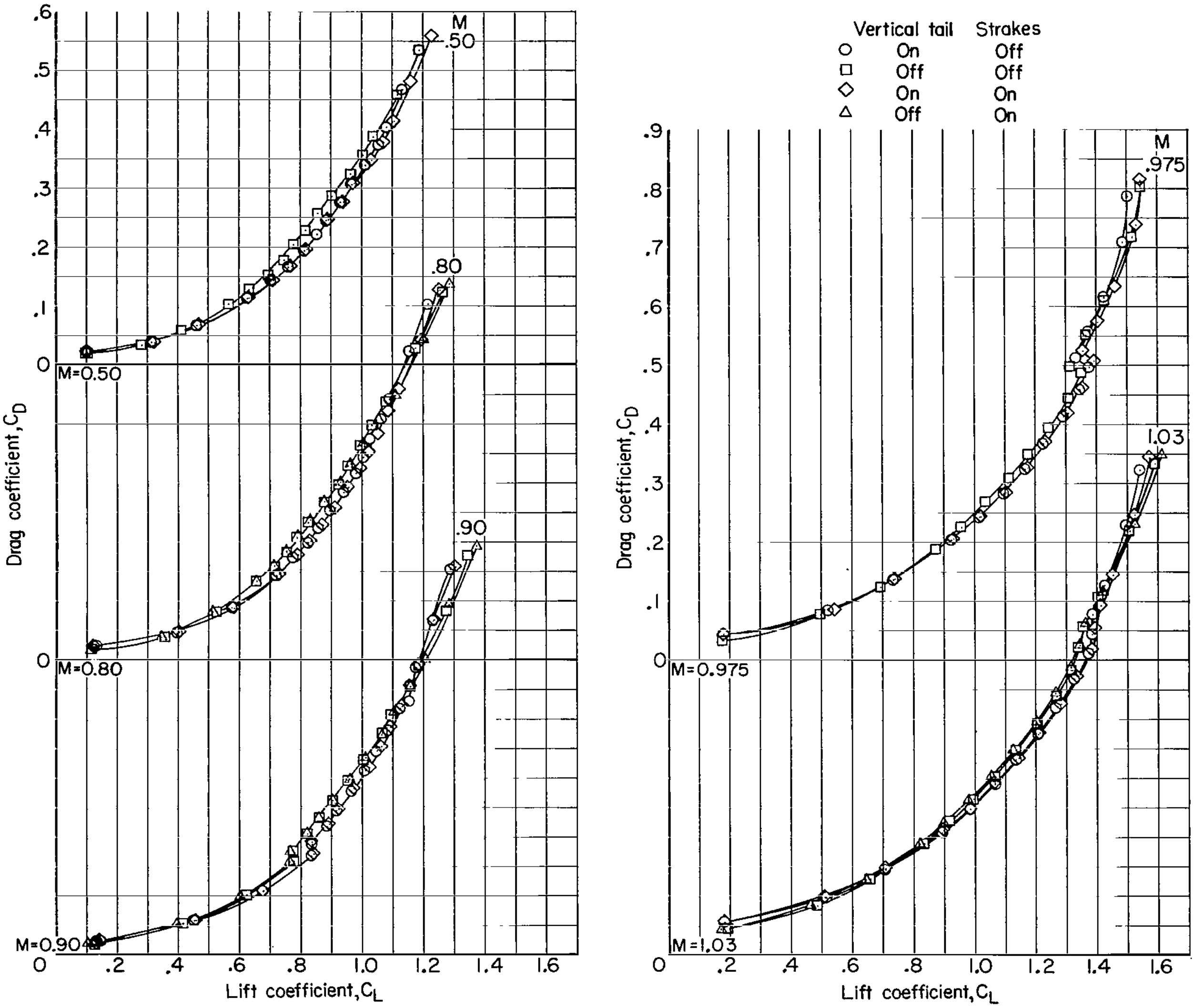

(b) Variation of C_D with C_L.

Figure 8.- Continued.

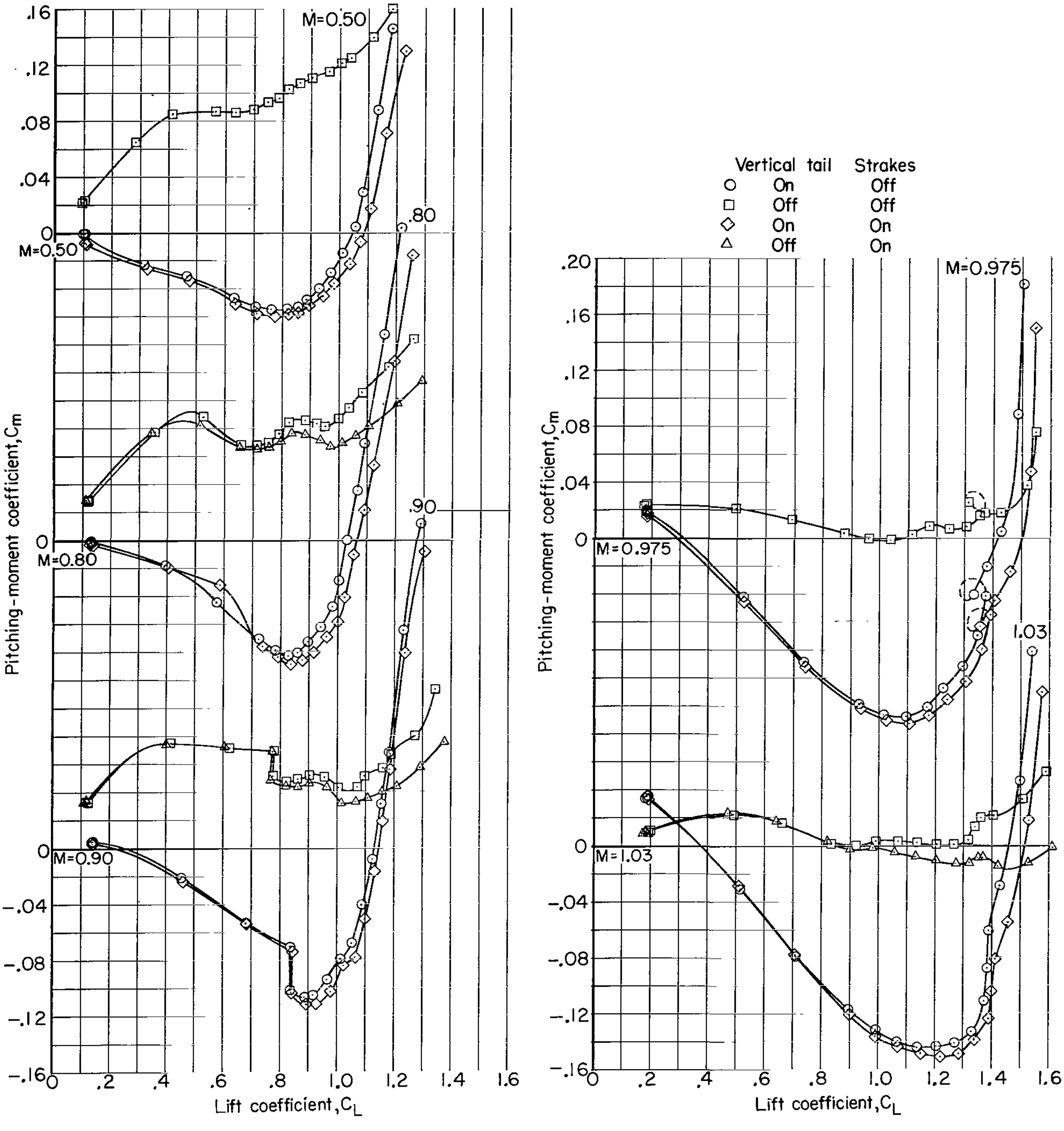

(c) Variation of C_m with C_L.

Figure 8.- Concluded.

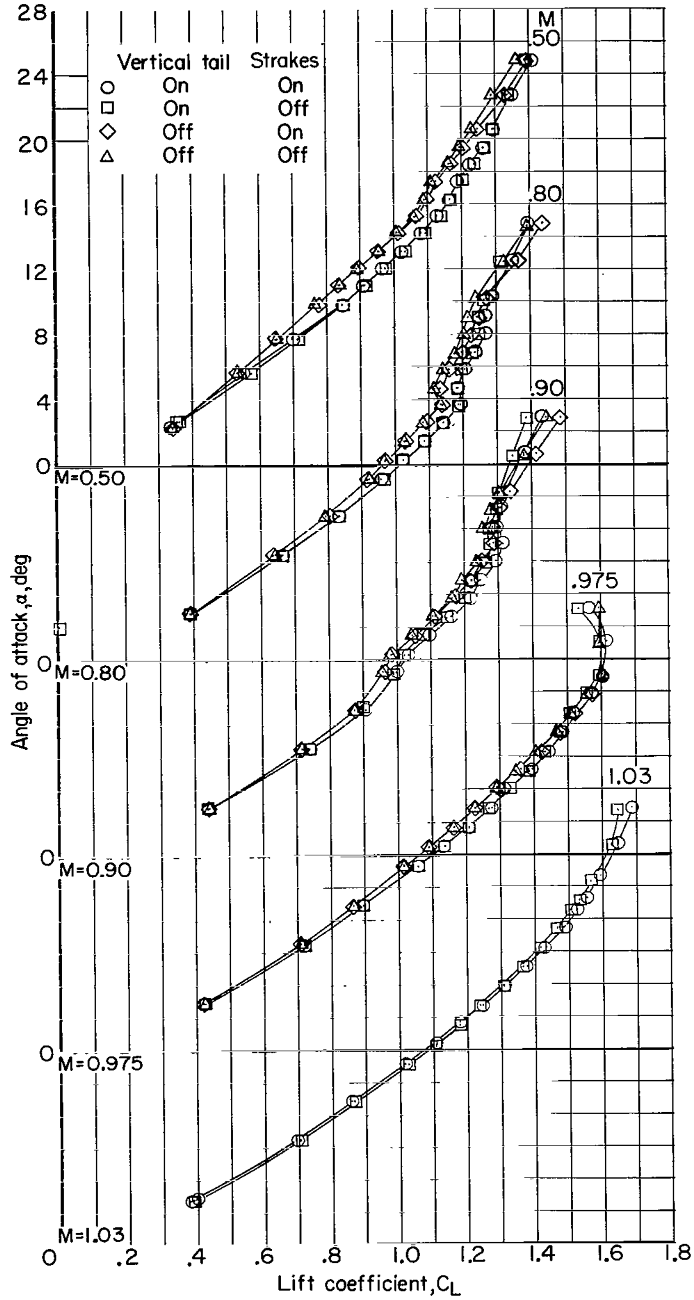

(a) Variation of α with C_L.

Figure 9.- Effects of the vertical tail and strakes on the aerodynamic characteristics of the configuration with leading-edge and trailing-edge flaps deflected 15^0. $\beta = 0^0$.

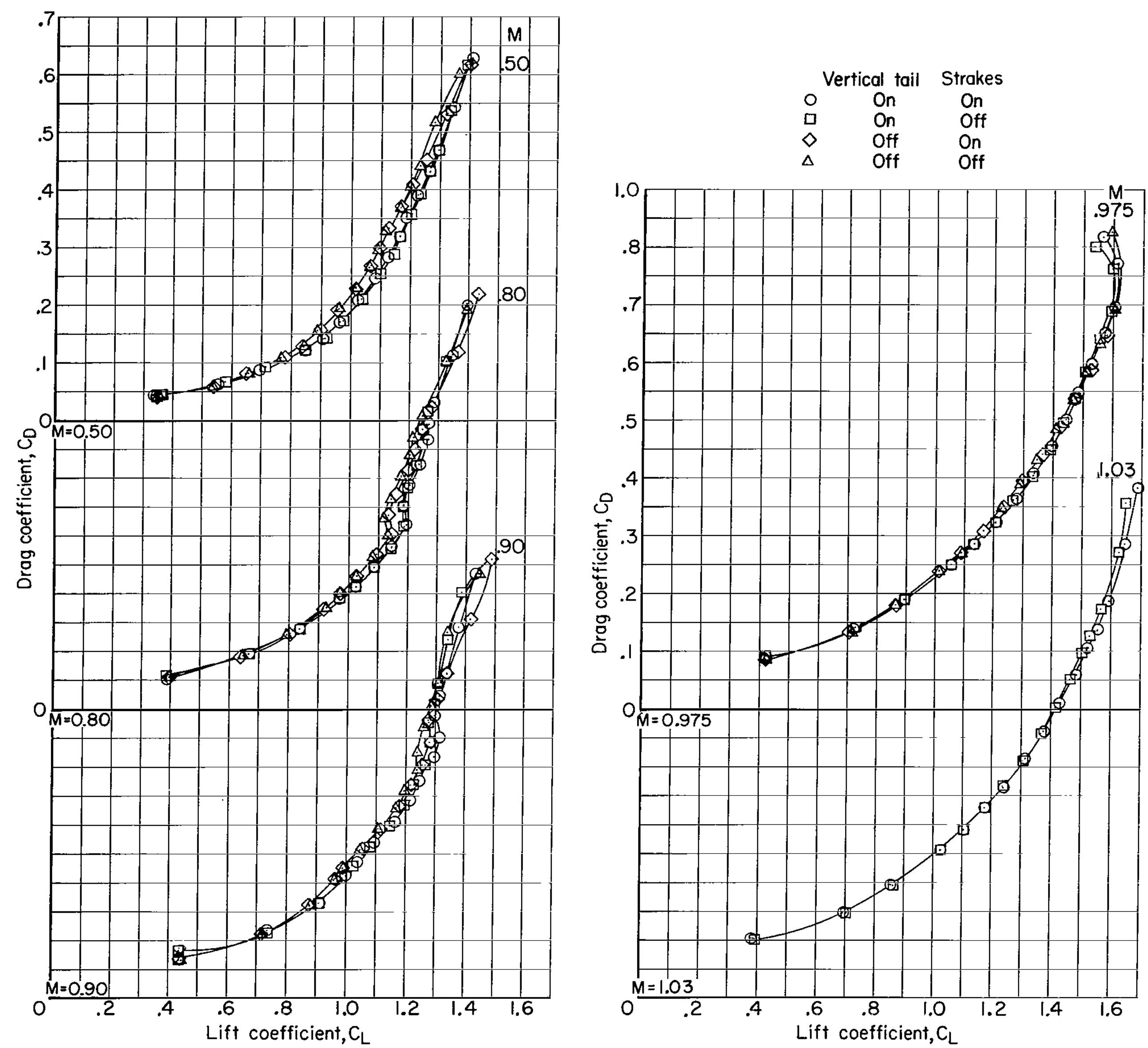

(b) Variation of C_D with C_L.

Figure 9.- Continued.

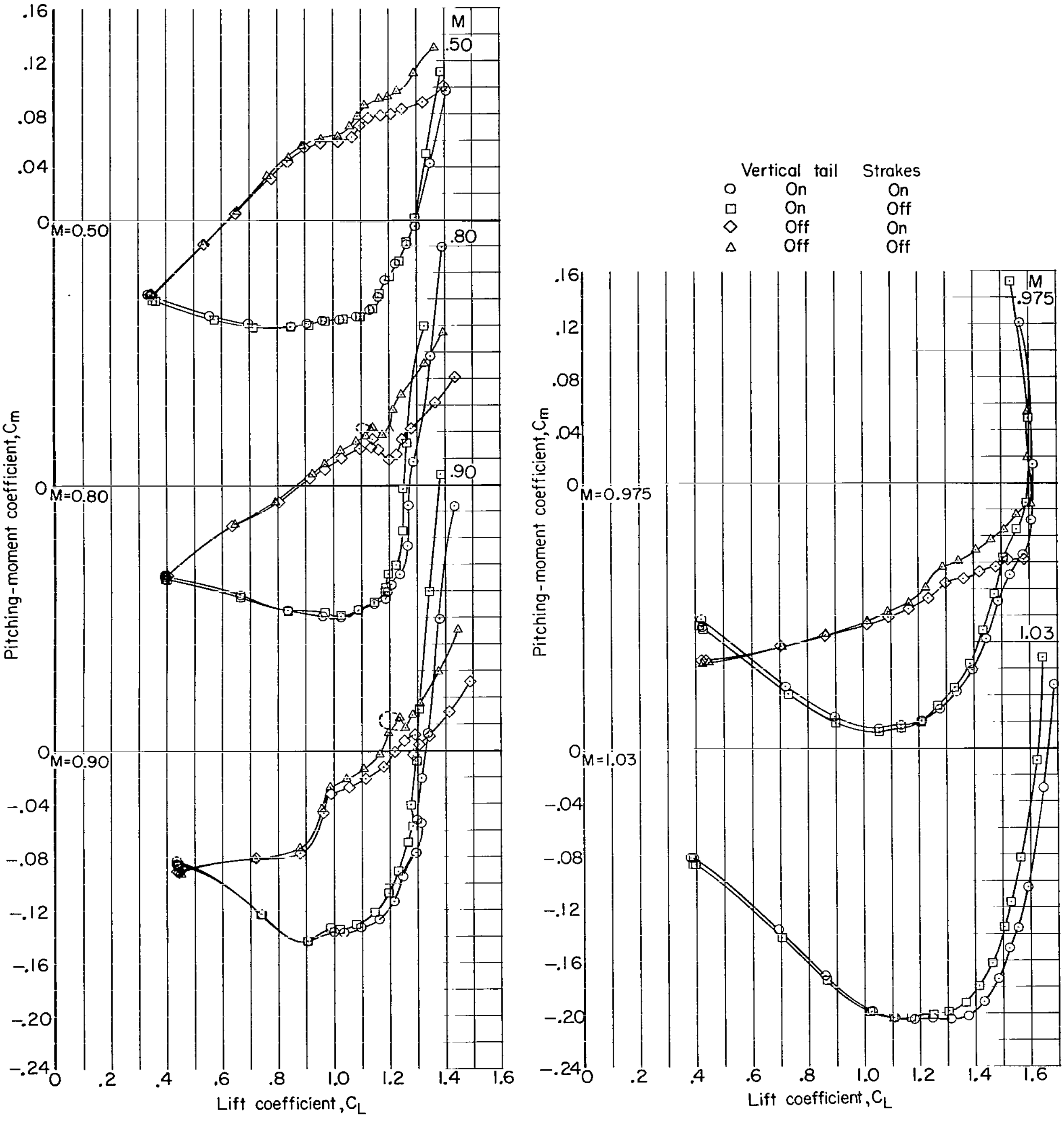

(c) Variation of C_m with C_L.

Figure 9.- Concluded.

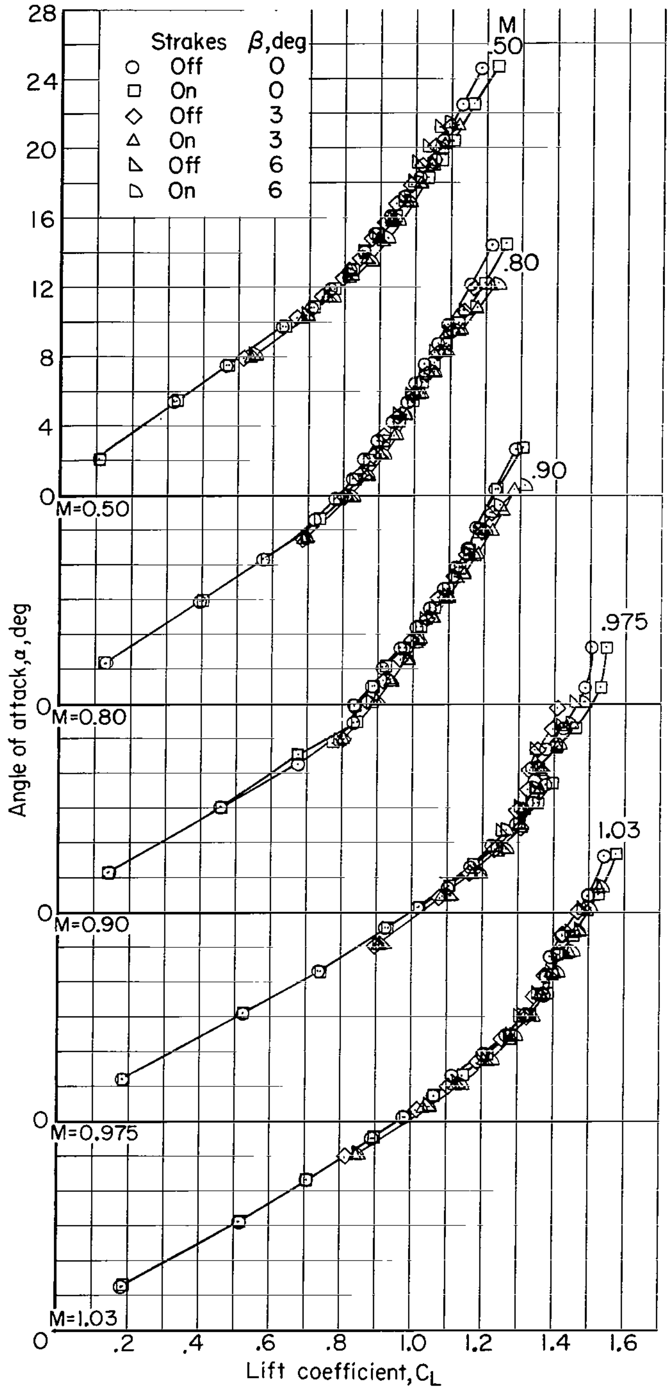

(a) Variation of α with C_L.

Figure 10.- Effect of sideslip angle on the aerodynamic characteristics of the strakes-on and strakes-off configurations with flaps neutral.

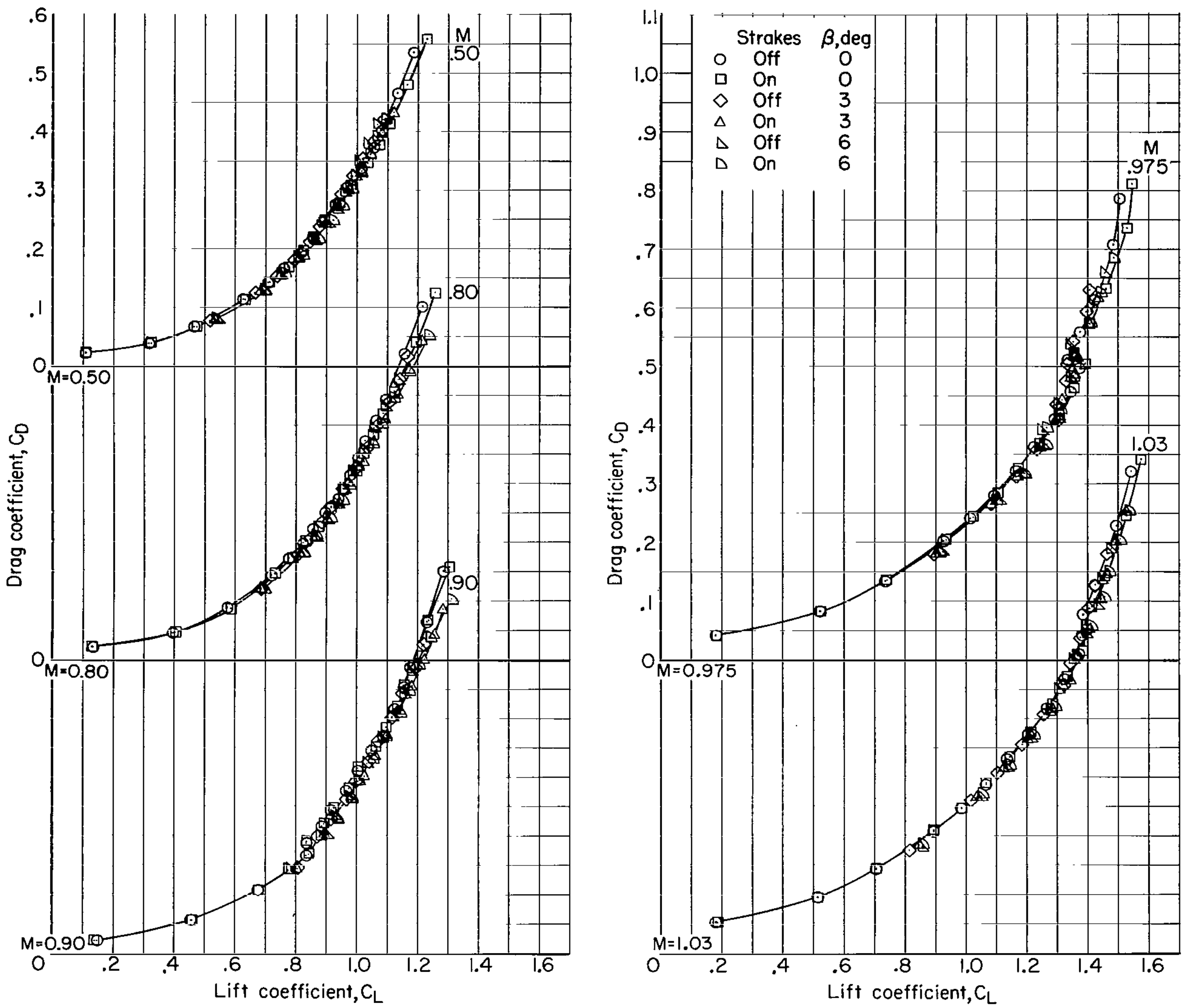

(b) Variation of C_D with C_L.

Figure 10.- Continued.

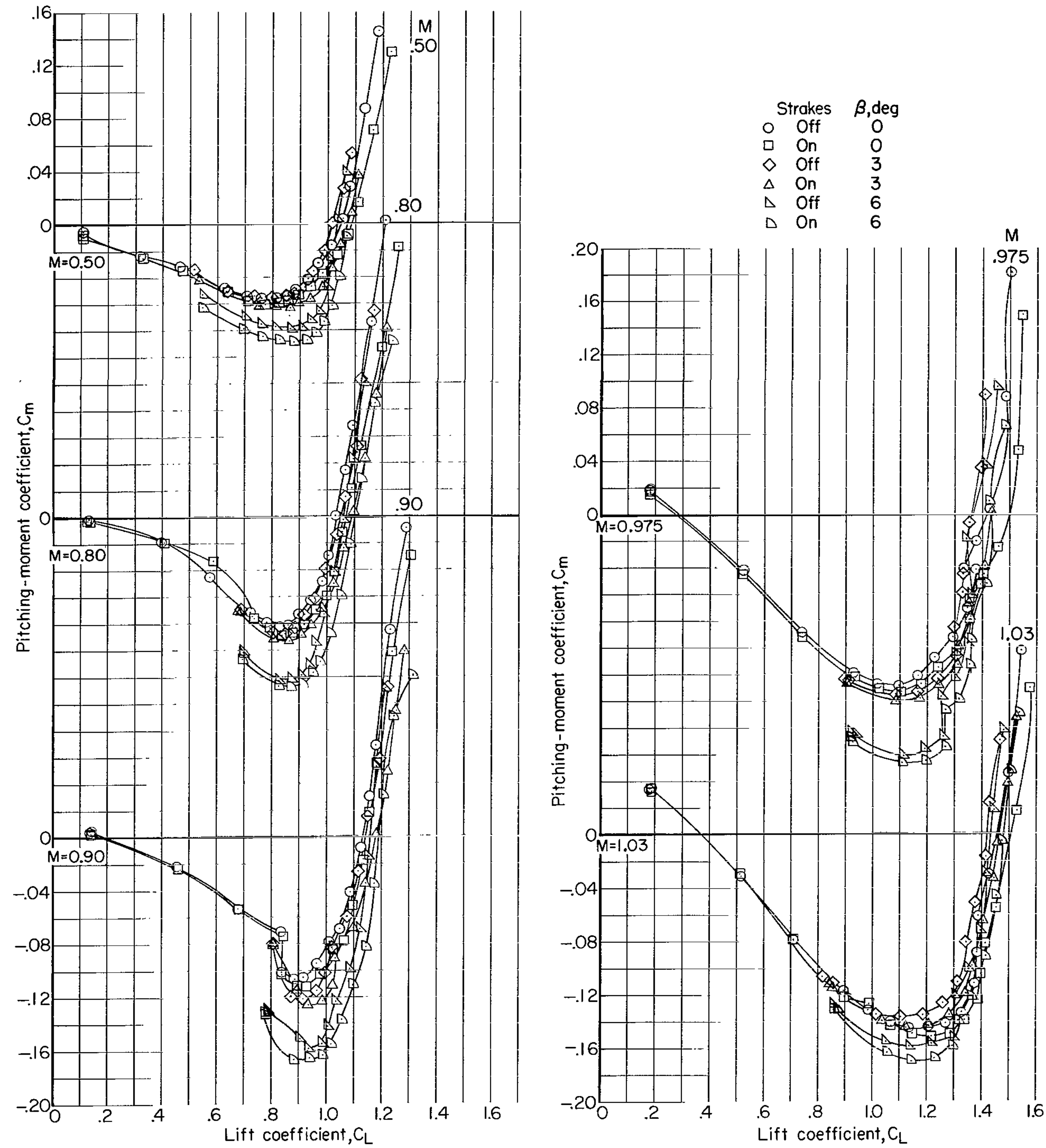

(c) Variation of C_m with C_L.

Figure 10.- Continued.

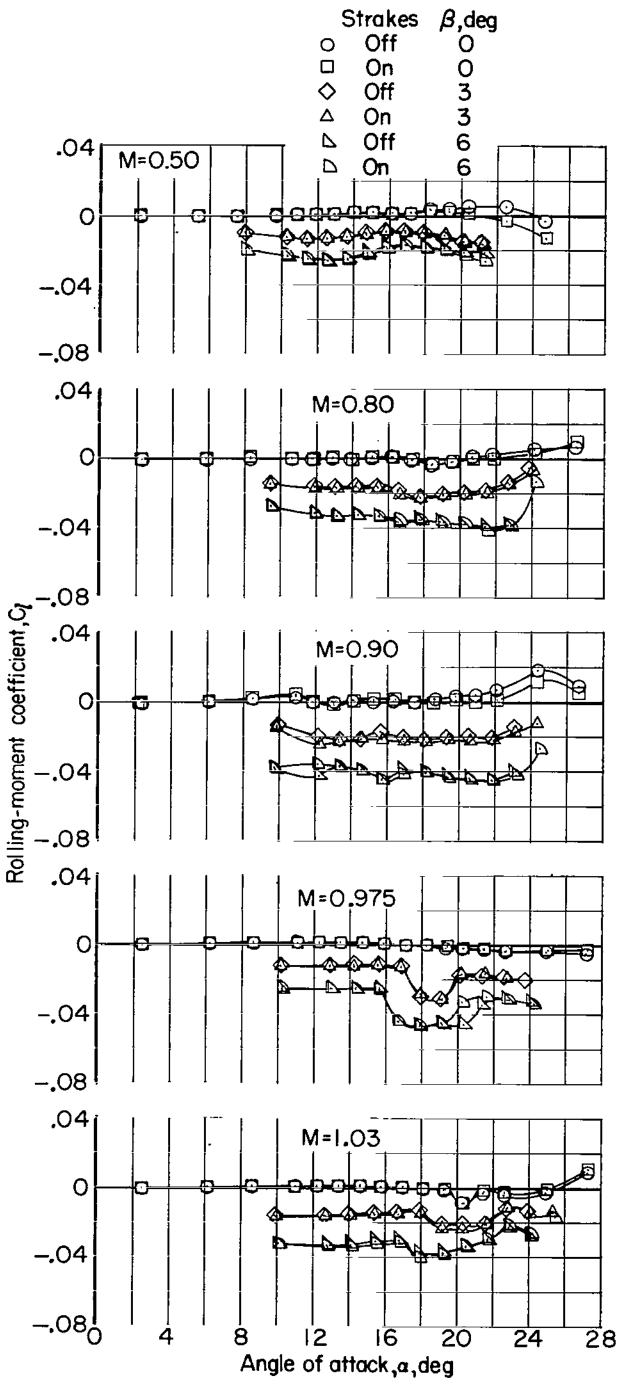

(d) Variation of C_l with α.

Figure 10.- Continued.

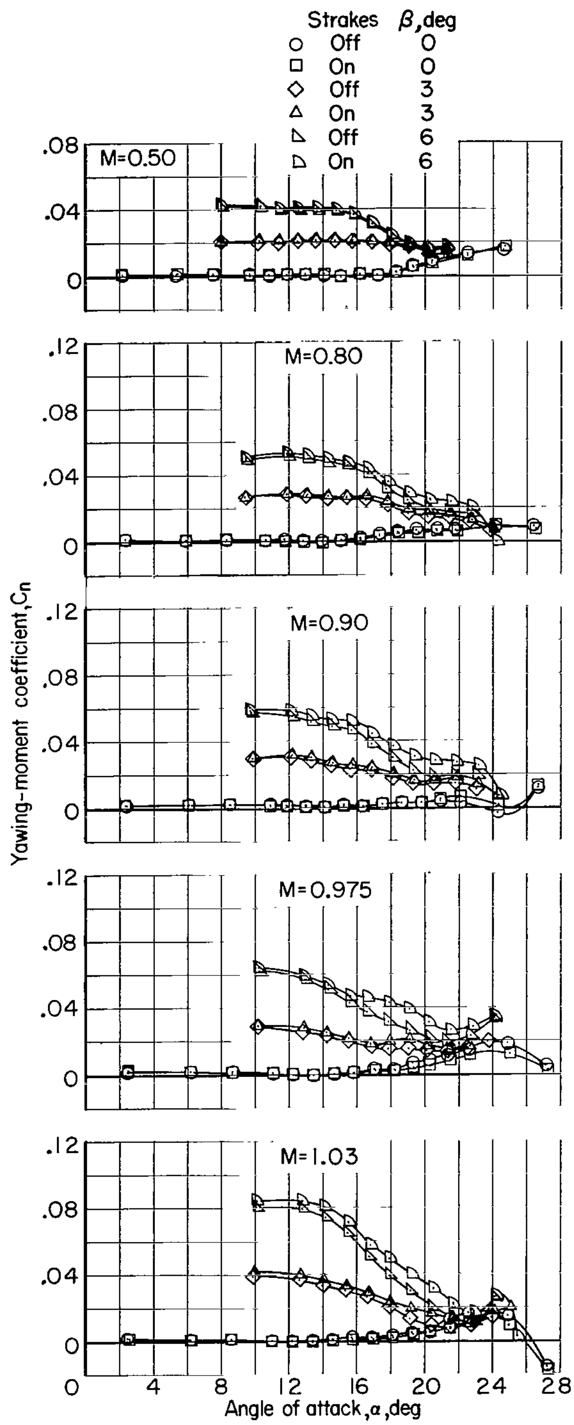

(e) Variation of C_n with α.

Figure 10.- Continued.

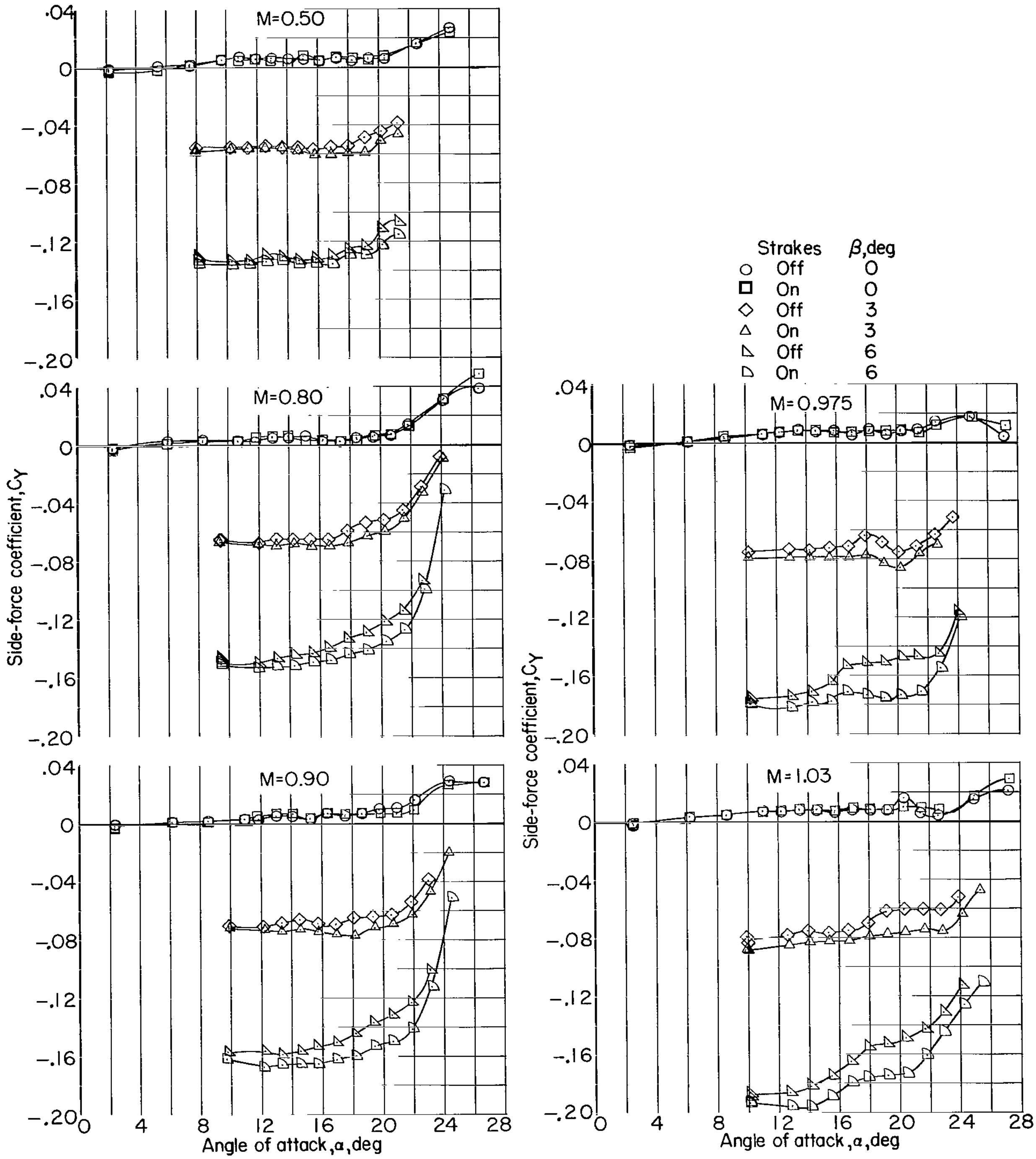

(f) Variation of C_Y with α.

Figure 10.- Concluded.

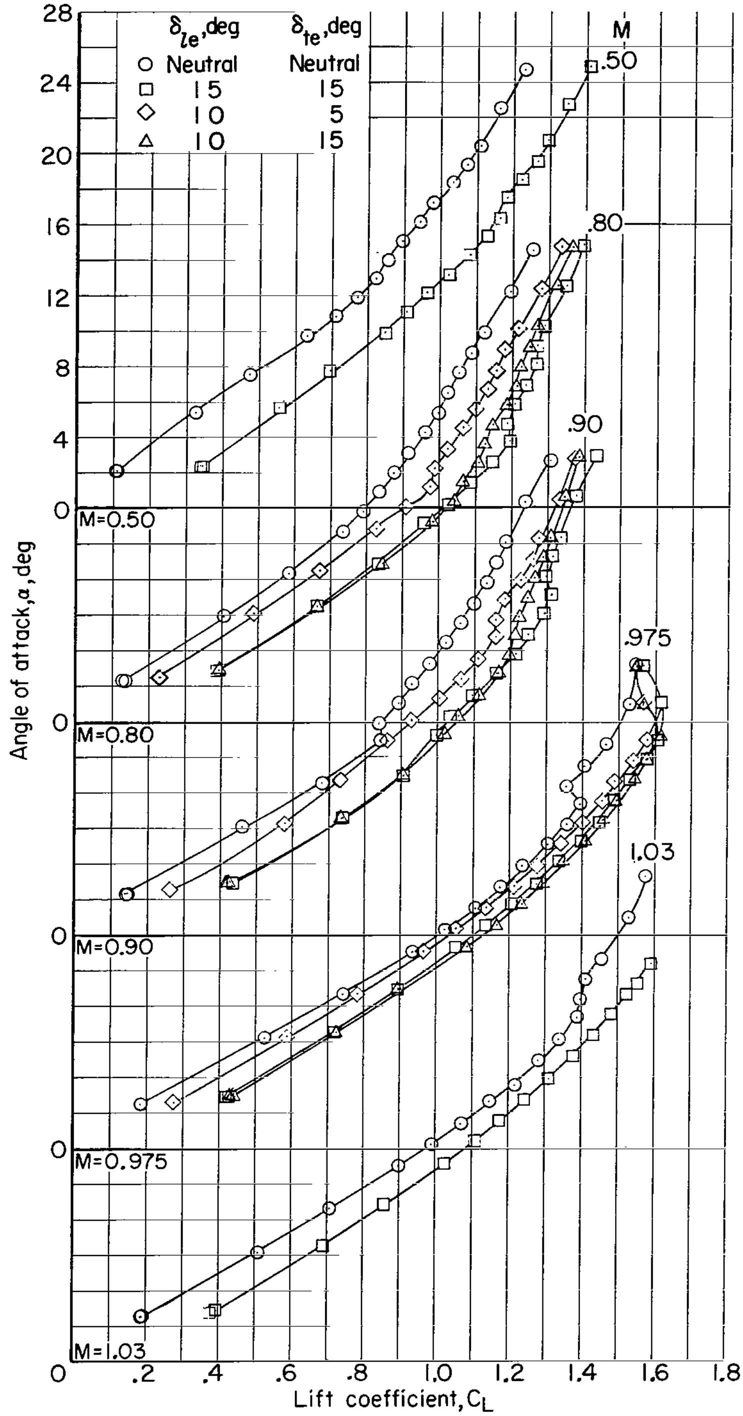

(a) Variation of α with C_L.

Figure 11.- Effect of leading-edge and trailing-edge flap deflections on the aerodynamic characteristics of the strakes-on configuration. $\beta = 0^{0}$.

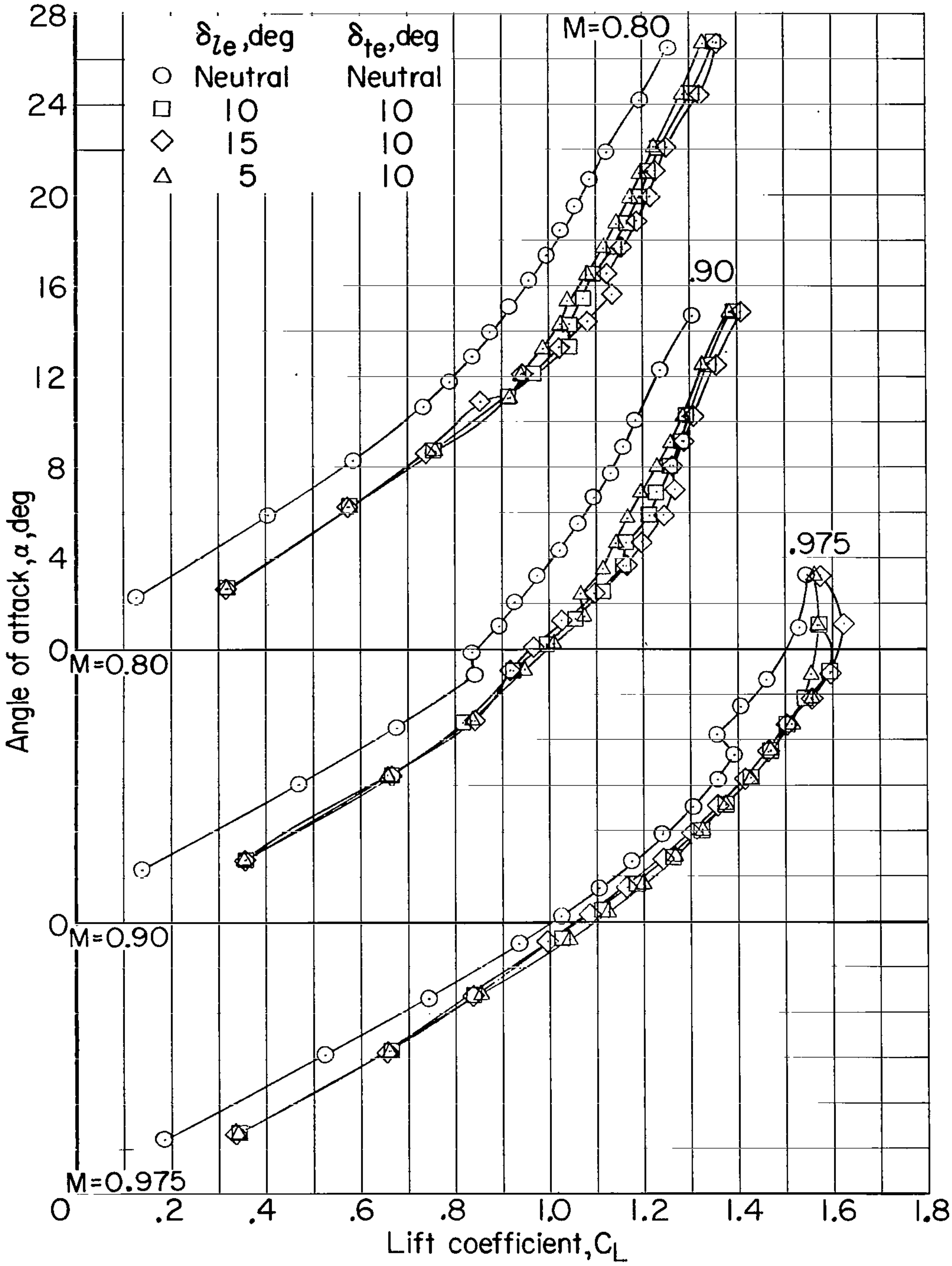

(a) Variation of α with C_L. Concluded.

Figure 11.- Continued.

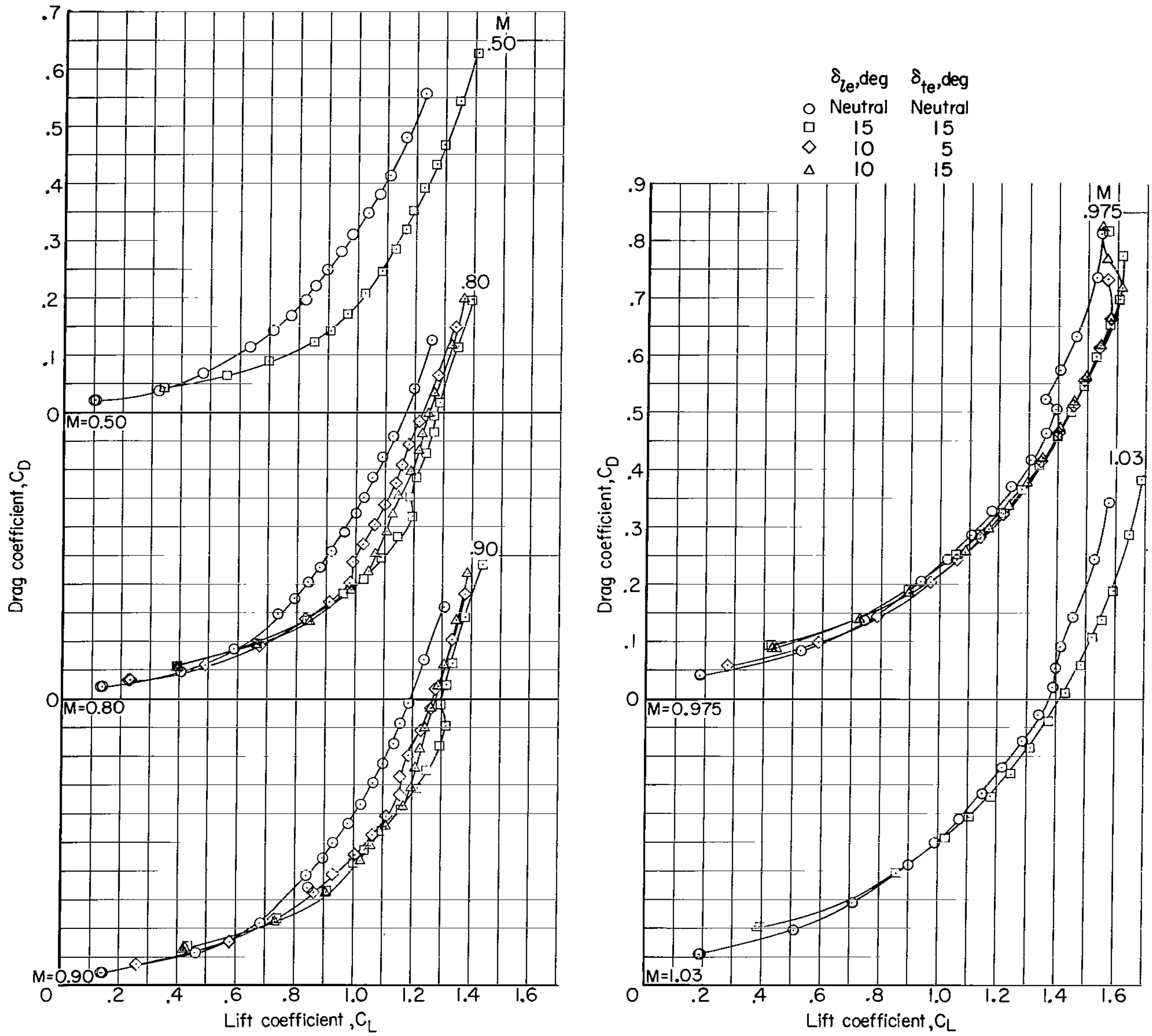

(b) Variation of C_D with C_L.

Figure 11.- Continued.

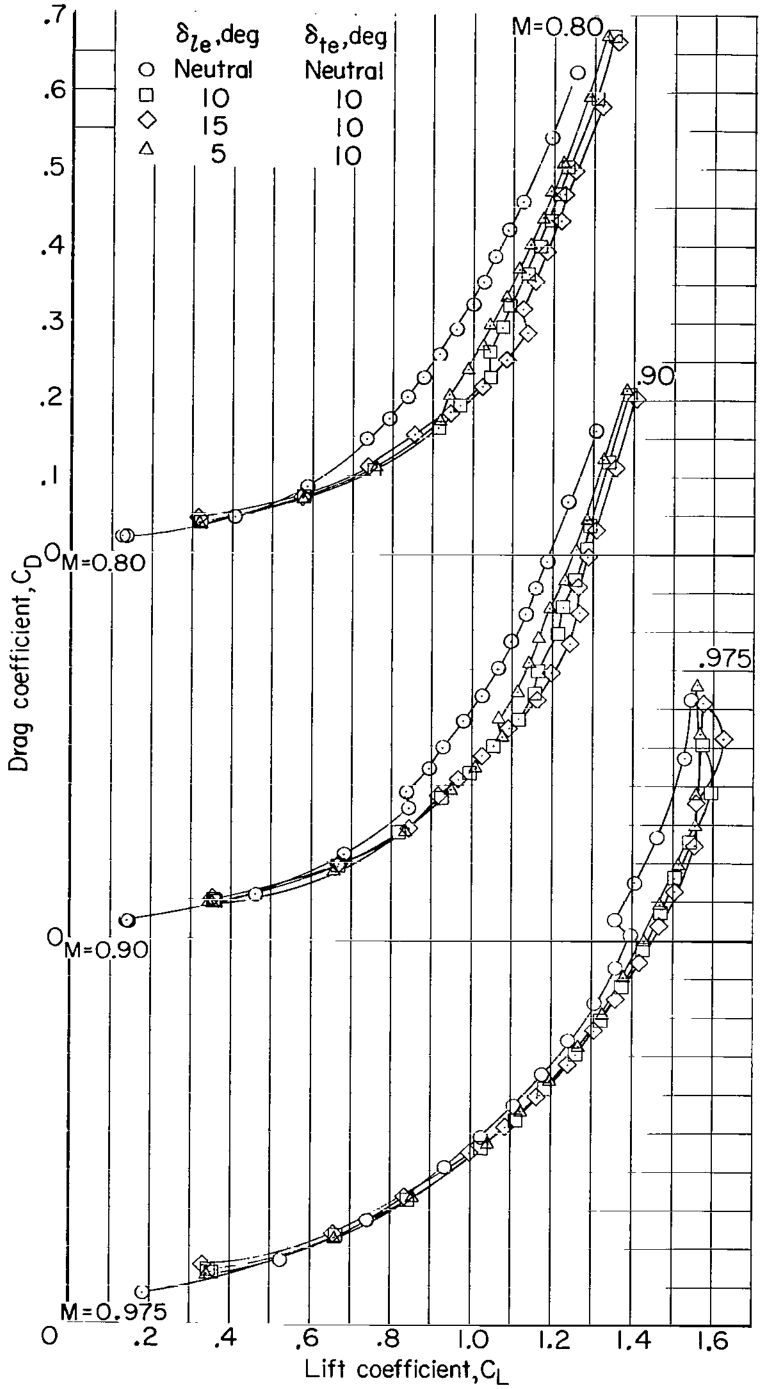

(b) Variation of C_D with C_L. Concluded.

Figure 11.- Continued.

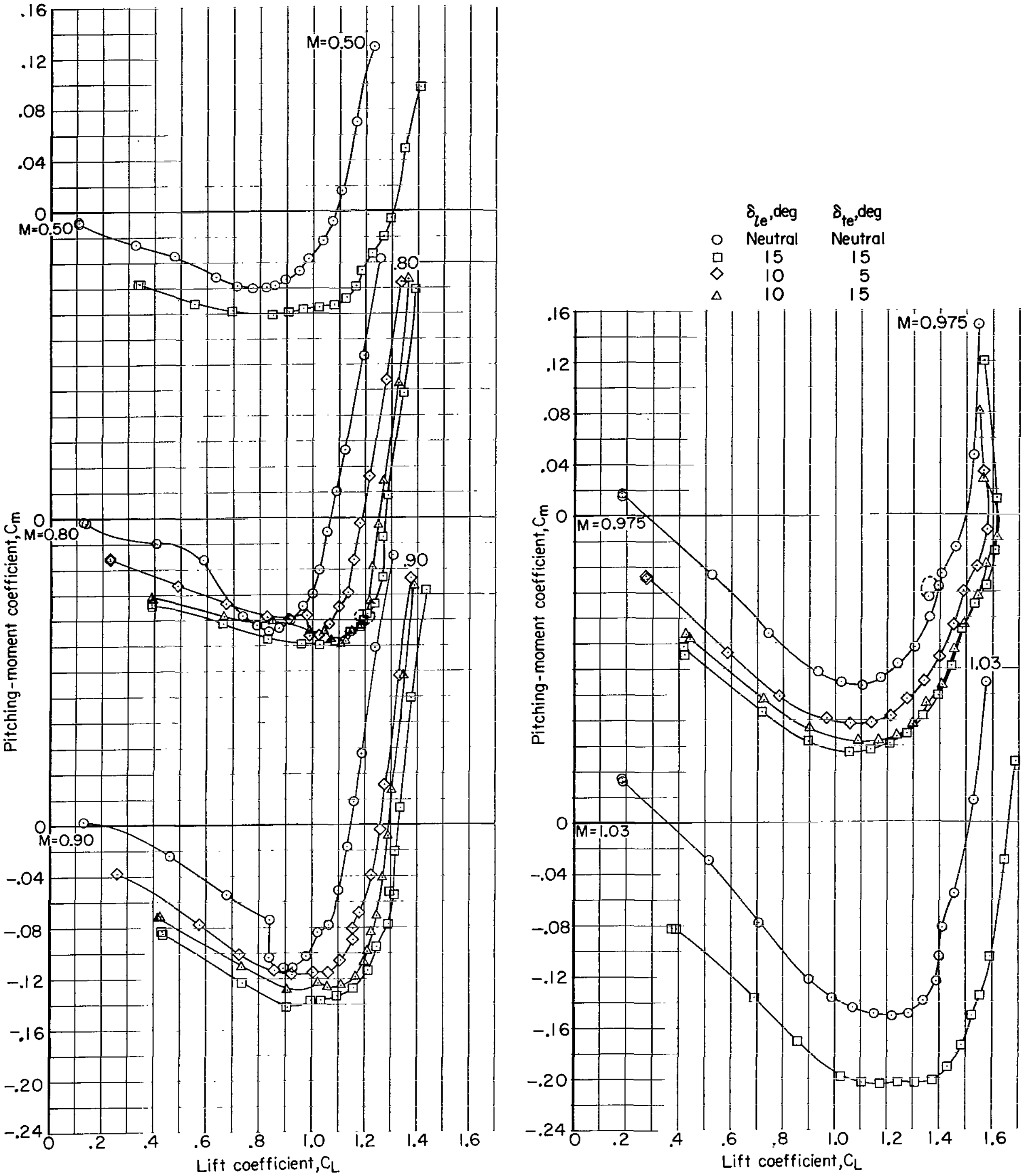

(c) Variation of C_m with C_L.

Figure 11.- Continued.

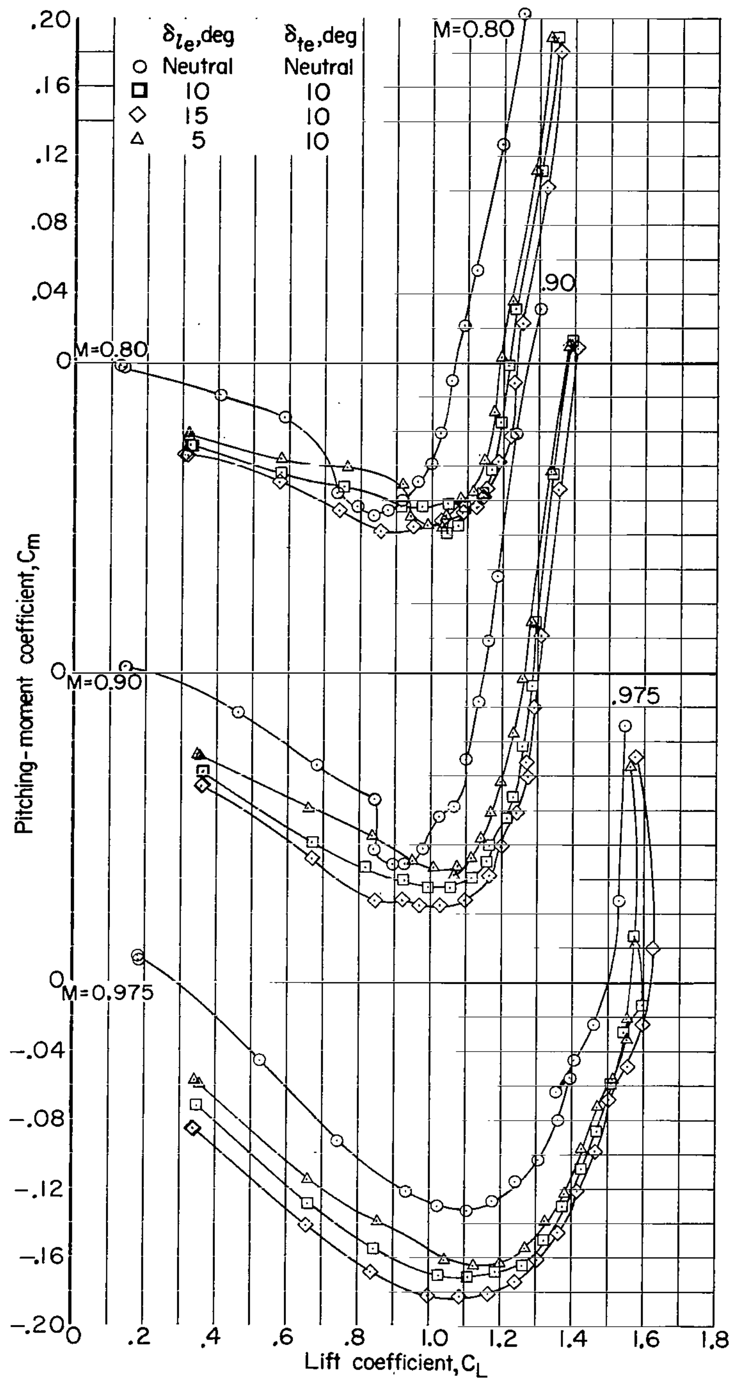

(c) Variation of C_m with C_L. Concluded.

Figure 11.- Concluded.

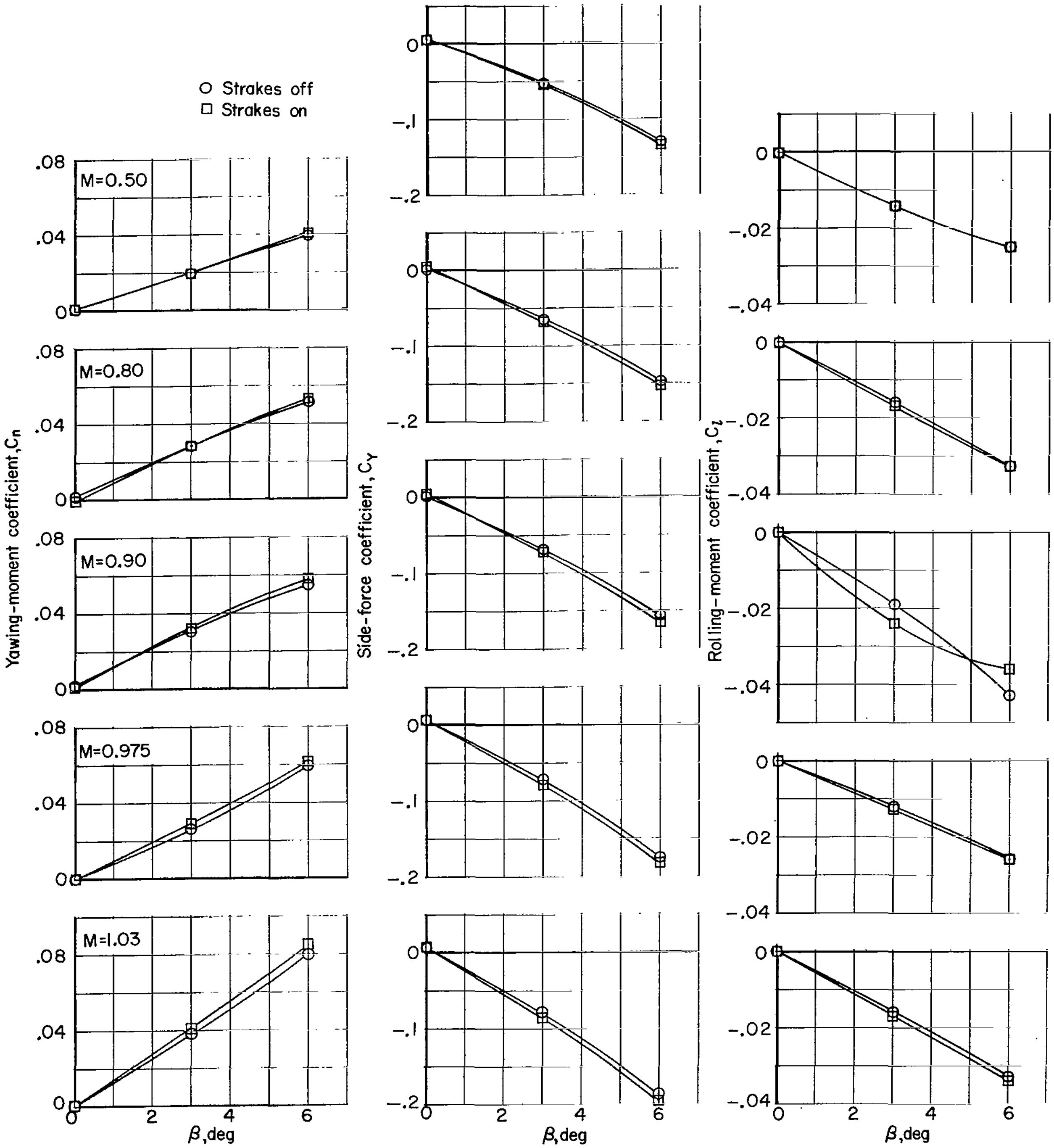

Figure 12.- Effect of strakes on the variation of yawing-moment, side-force, and rolling-moment coefficients with angle of sideslip. Flaps neutral; $\alpha = 12^{0}$.

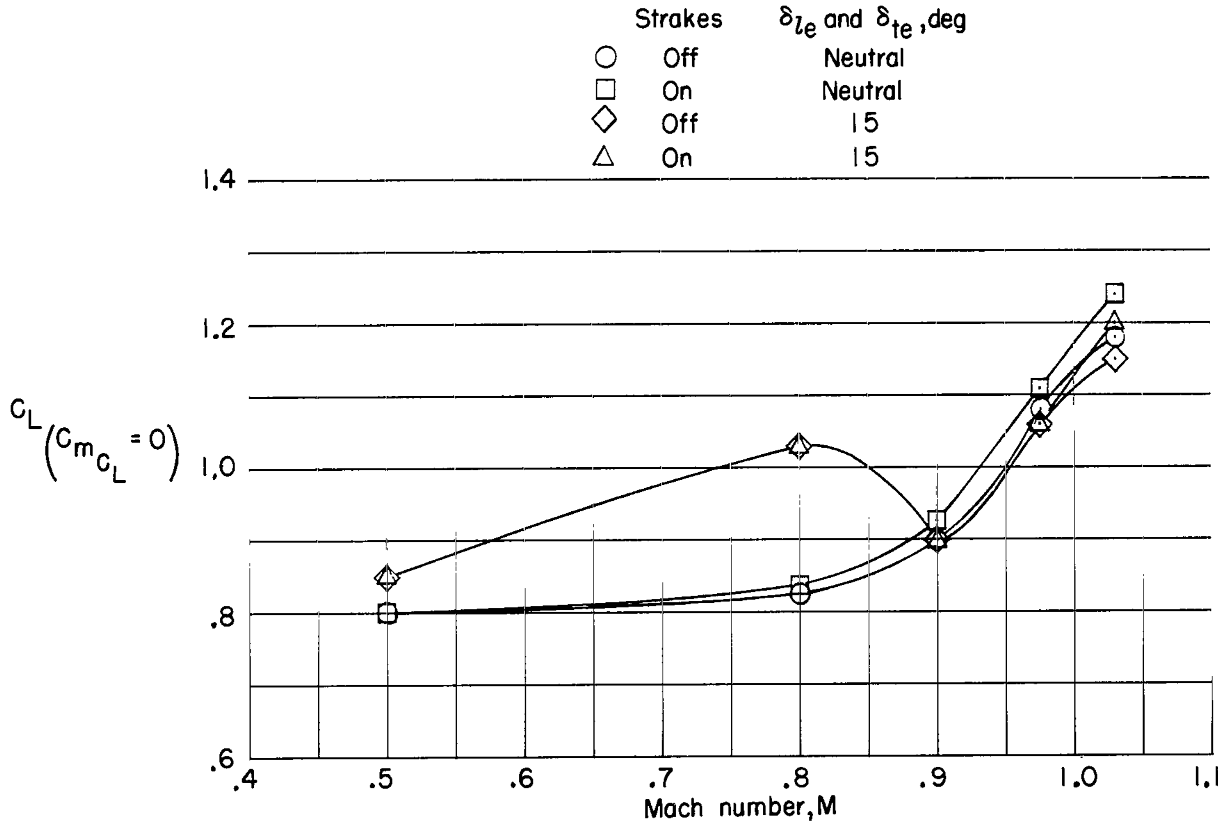

Figure 13.- Variation of the pitch-up lift coefficient with Mach number for the strakes-on and strakes-off configurations with flaps neutral and deflected 15^0.

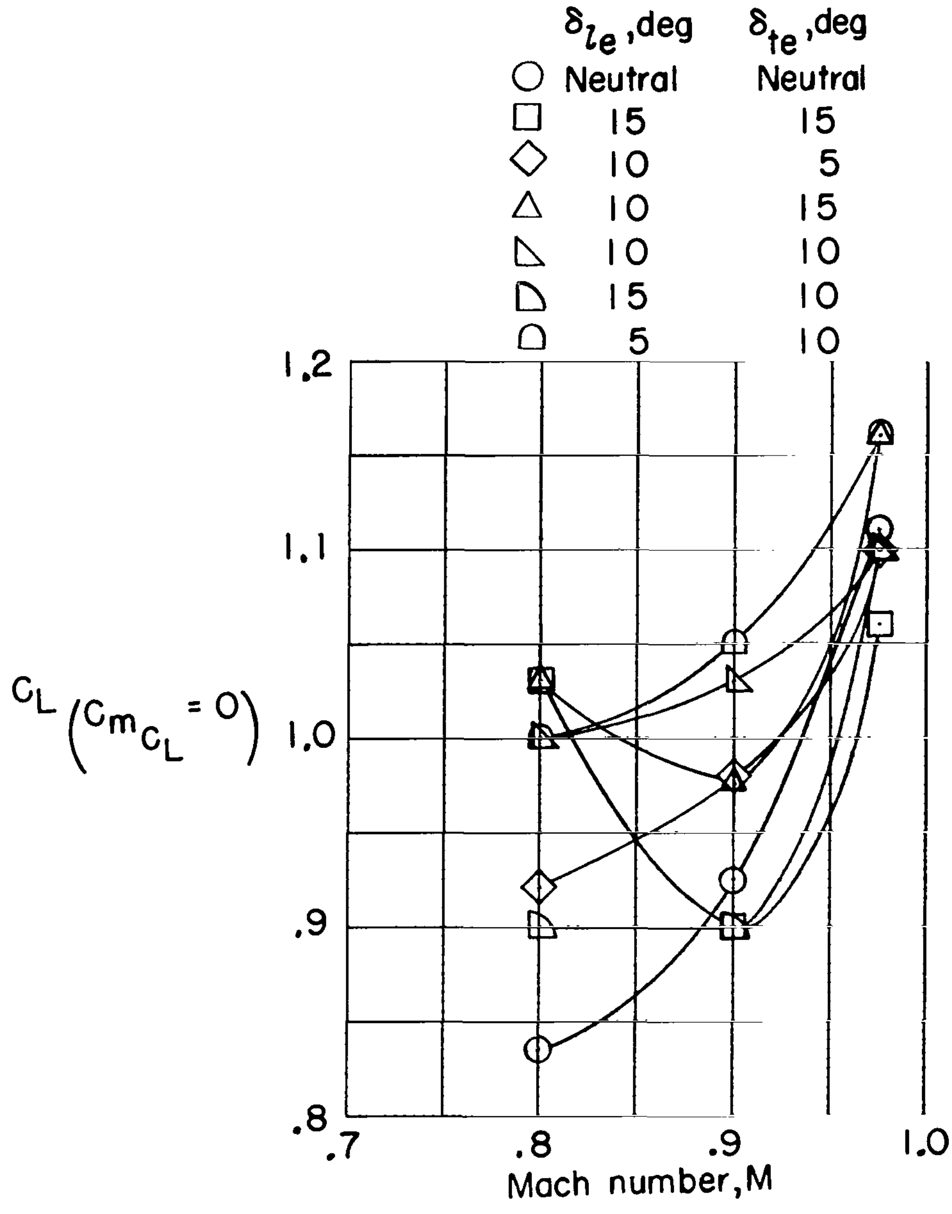

Figure 14.- Effect of various leading-edge and trailing-edge flap deflections on the variation of the pitch-up lift coefficient with Mach number for the strakes-on configuration.

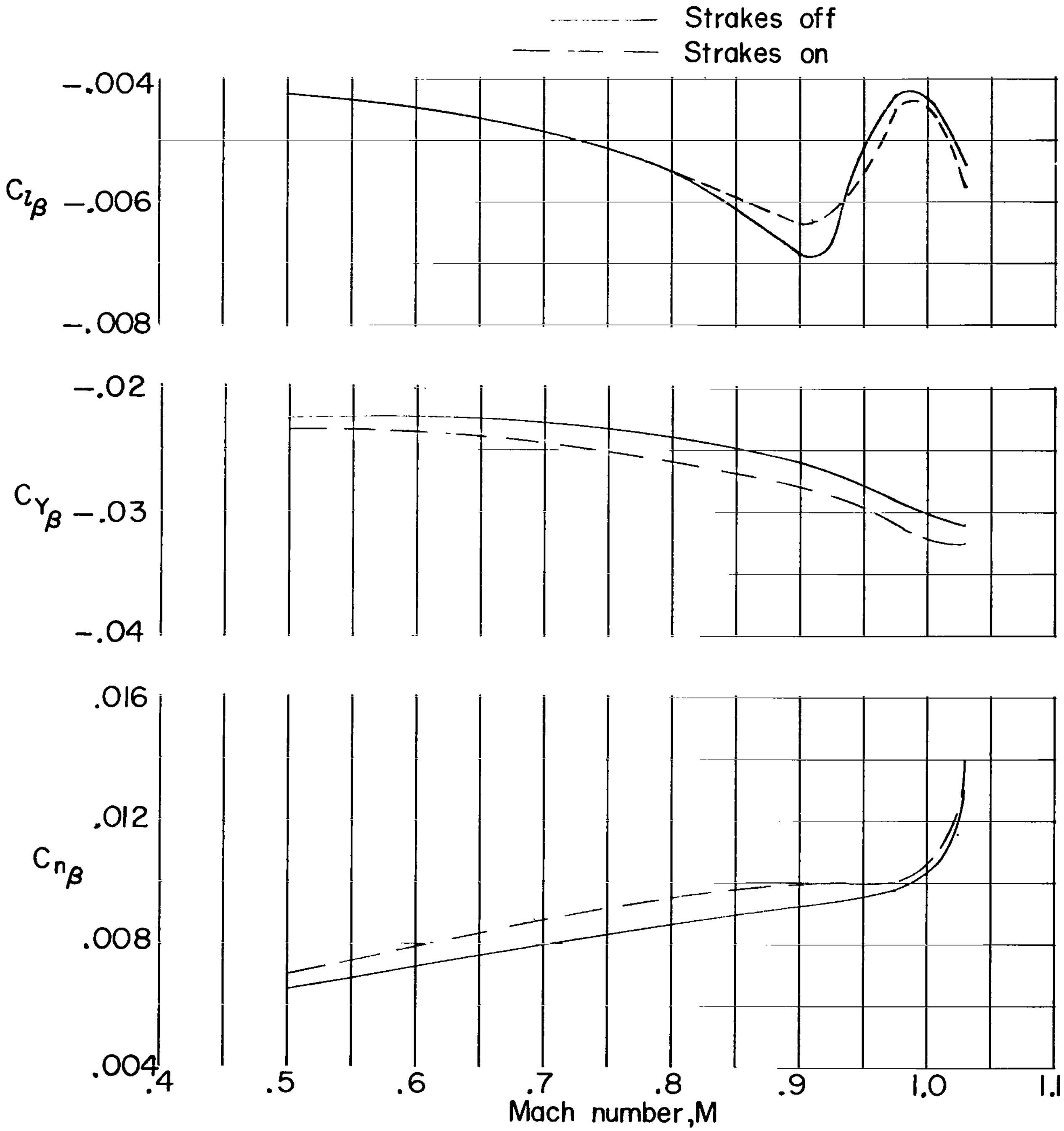

Figure 15.- Effect of strakes on the variation of sideslip derivatives with Mach number. $\alpha = 12^0$.

3/18/25 [illegible]

"The aeronautical and space activities of the United States shall be conducted so as to contribute . . . to the expansion of human knowledge of phenomena in the atmosphere and space. The Administration shall provide for the widest practicable and appropriate dissemination of information concerning its activities and the results thereof."

—NATIONAL AERONAUTICS AND SPACE ACT OF 1958

NASA SCIENTIFIC AND TECHNICAL PUBLICATIONS

TECHNICAL REPORTS: Scientific and technical information considered important, complete, and a lasting contribution to existing knowledge.

TECHNICAL NOTES: Information less broad in scope but nevertheless of importance as a contribution to existing knowledge.

TECHNICAL MEMORANDUMS: Information receiving limited distribution because of preliminary data, security classification, or other reasons.

CONTRACTOR REPORTS: Technical information generated in connection with a NASA contract or grant and released under NASA auspices.

TECHNICAL TRANSLATIONS: Information published in a foreign language considered to merit NASA distribution in English.

TECHNICAL REPRINTS: Information derived from NASA activities and initially published in the form of journal articles.

SPECIAL PUBLICATIONS: Information derived from or of value to NASA activities but not necessarily reporting the results of individual NASA-programmed scientific efforts. Publications include conference proceedings, monographs, data compilations, handbooks, sourcebooks, and special bibliographies.

Details on the availability of these publications may be obtained from:

SCIENTIFIC AND TECHNICAL INFORMATION DIVISION

NATIONAL AERONAUTICS AND SPACE ADMINISTRATION

Washington, D.C. 20546